DYNAMICS AND CONTROL OF AN ELECTRIC POWER

ASSIST STEERING SYSTEM

PRASANTH BABU KANDULA

Bachelor of Electrical and Communication Engineering

Jawaharlal Nehru Technological University

MAY, 2006

Submitted in partial fulfillment of requirements for the degree

MASTER OF SCIENCE IN ELECTRICAL ENGINEERING

at the

CLEVELAND STATE UNIVERSITY

AUGUST, 2010

This thesis has been approved

for the Department of Electrical and Computer Engineering

and the College of Graduate Studies by

_____

Thesis Committee Chairperson, Lili Dong

_____

Department/Date

_____

Committee Member, Zhiqiang Gao

_____

Department/Date

_____

Committee Member, Wenbing Zhao

_____

Department/Date

ACKNOWLEDGEMENT

DYNAMICS AND CONTROL OF AN ELECTRIC POWER ASSIST STEERING SYSTEM

PRASANTH BABU KANDULA

ABSTRACT

In this thesis an Active Disturbance Rejection Controller (ADRC) is applied to Electrical Power Assist Steering (EPAS) system which assists the driver in steering the steering wheel of an automobile. Our control objective is to reduce the steering torque exerted by a driver, so that good steering feel of the driver will be achieved in the presence of external disturbances and system uncertainties which are very common in the EPAS system. The robustness and stability of ADRC controlled EPAS system is investigated through frequency-domain analyses. The Bode diagrams and stability margins demonstrate that the control system is stable during the operation and it is robust against external disturbances and structural uncertainties. In addition, the ADRC is simulated on a column-type EPAS system. The simulation results show that using the proposed ADRC, the driver can turn the steering wheel with the desired steering torque, which is independent of load torques that tend to vary with the change of driving conditions.

TABLE OF CONTENTS

Page No.

NOMENCLATURE

EPAS: Electrical Power Assist Steering system

HPS: Hydraulic Power Assist Steering System

ADRC: Active Disturbance Rejection Controller

ESO: Extended State Observer

PI: Proportional-Integral Controller

PD: Proportional-Derivative Controller

PID: Proportional-Integral-Derivative Controller

EPS-TT: Column-type Electric Power Steering

ODE: Ordinary Differential Equation

LIST OF TABLES

Table Title

LIST OF FIGURES

Figure Title

x

CHAPTER I

INTRODUCTION

This chapter introduces background knowledge of steering systems and discusses different types of gear units used in the steering systems. The chapter also explains power steering and its different kinds. Then an electric power assist steering system (EPAS) is elaborated. The existing controller designs for the EPAS are discussed. Finally the contributions and outline of this thesis are stated.

1.1 Introduction to steering system

The steering system is one of the major subsystems for vehicle operation [1]. Benz experienced difficulty in designing a satisfactory steering mechanism for a four-

wheeled vehicle and so his first cars were tricycles [2]. Even after 1900 there was at least one vehicle still being made with center pivot steering [2] while center pivot steering is a steering system often used in tricycles. For a tricycle, steering control arm is center mounted on the steering shaft as shown in Figure 1. The arm is turned to change the direction of the vehicle. The American manufactures initially applied power assistance to car steering in quantity production [3]. In 1926, power steering system, which is a steering mechanism in which driver is assisted my external force to drive the vehicle, was first introduced by F W Davis to automobiles but was unfortunately rejected due to depression [2]. Acceptance of power steering by automobile industry was slow at beginning. But by 1966 it had been used in about a third of American cars and by 1978 in more than 90% [2] of American cars.
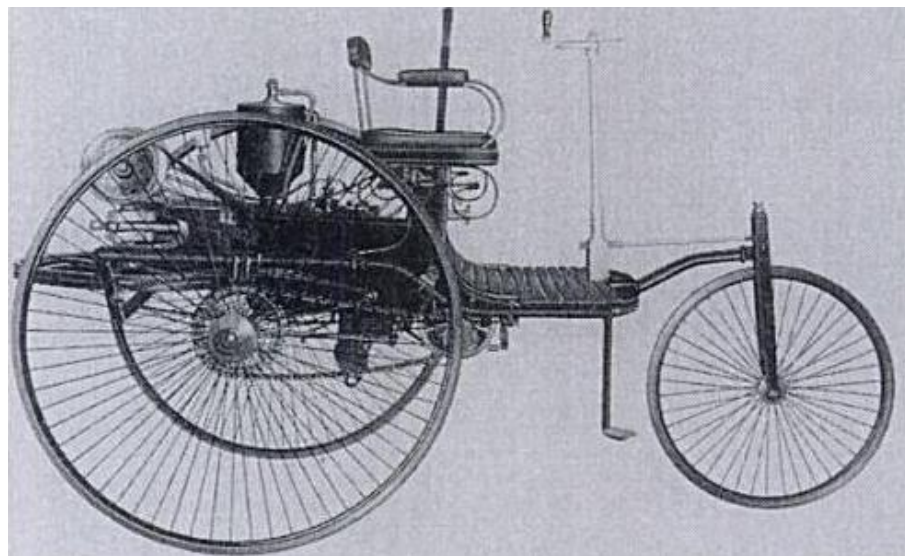
Figure 1:   Benz tricycle [4]

1.2   Background

A steering wheel is generally positioned in front of the driver who has to apply some torque to rotate the steering wheel to steer the vehicle wheels. Steering will convert the rotary motion of a steering wheel to the turn motion of the vehicle's steered wheels. Front wheel steering is the most common steering method used in these days.

The modern steering system consists of two major units, a gear unit and a steering column [5]. The steering column is a shaft which connects the steering wheel to gear unit. In modern automobiles steering column is designed to collapse in collision to protect driver [5]. The gear unit is a unit which translates the rotational force applied to steering shaft into required form. There are four major types of gear units in modern cars. They are worm-sector, worm- roller, re-circulating ball nut, and rack and pinion. The details of theses four types of gear units are given in the following paragraph. In this thesis, we will use rack and pinion steering gear since it is widely used in small automobiles.

A worm-sector is a type of gear unit where the worm is connected to steering shaft. When the steering shaft is rotated it will rotate the worm around its axis causing the sector to rotate. The pitman arm which is connected to sector and steering linkage will turn the vehicle wheels in order to govern the vehicle direction. Figure 2 shows the mechanical model of the worm-sector gear.
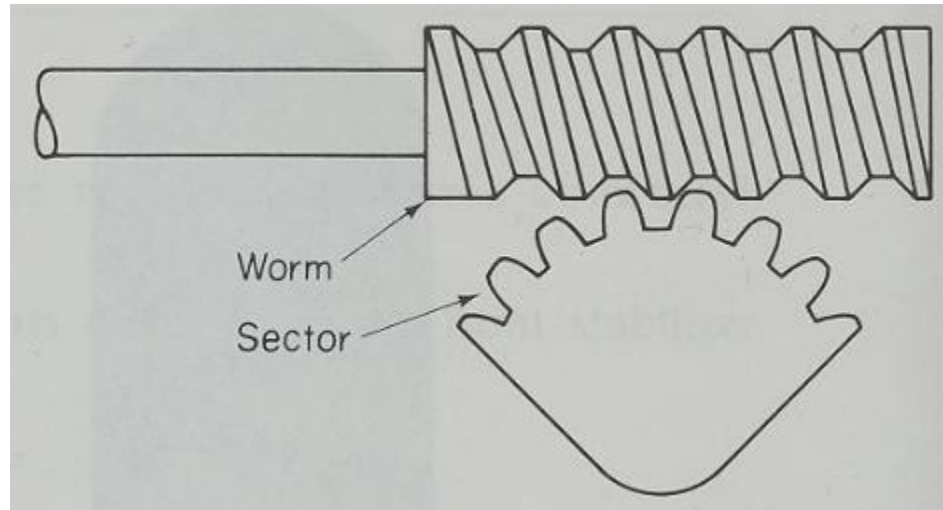
Figure 2: Worm-sector gear [5]

A worm-roller is another kind of gear unit which is similar to worm sector in the worm part. The difference between worm-roller and worm-sector gear units is that the sector is replaced with the roller. The worm rotates the roller which displaces the steering linkage to drive the wheels in necessary direction. Figure 3 shows the mechanical model of the worm-roller gear.
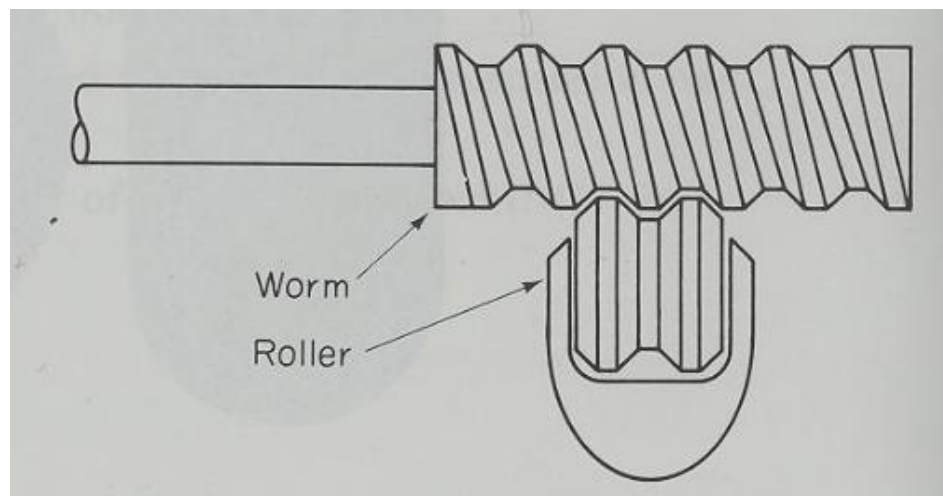
Figure 3: Worm-roller gear [5]

4

Re-circulating ball nut is also a kind of worm sector gear unit. In re-circulating ball nut, the worm is rotated by steering shaft. The block of the worm gear has a threaded hole and a gear teeth cut into the outside of the block to move the sector. When the worm is rotated, instead of moving further into the block since the worm is fixed, it will displace the block. The displaced block will turn the sector via gear teeth. Finally, the sector will move the pitman arm and pass through that steering linkage. The threads are filled with ball bearings which will re-circulate when the block is moved. Figure 4 shows the mechanical model of the re-circulating ball nut steering gear unit.
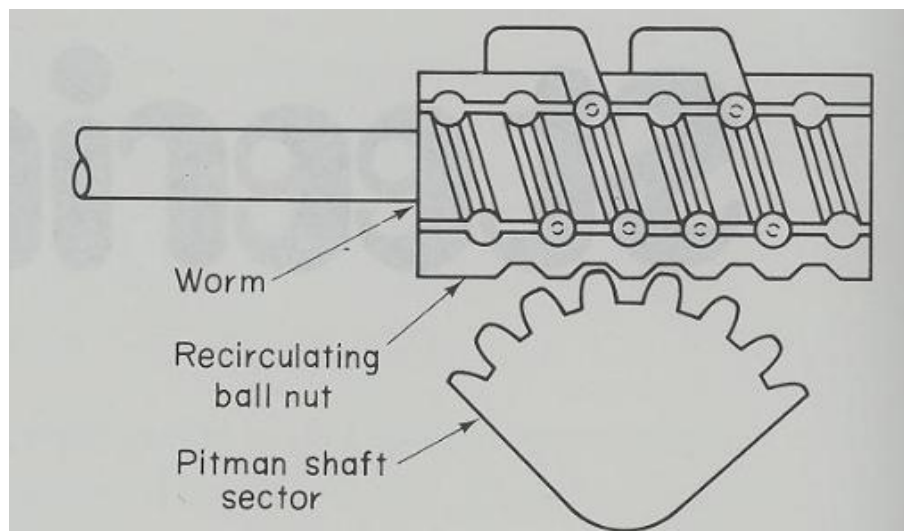
Figure 4: Recirculating ball nut gear [5]

In Figure 5, a rack-and-pinion gear is given. In the figure, the rack and pinion is simple, light and responsive [5]. The pinion, controlled by steering wheel via steering column, has teeth that engage with the teeth of the rack [5]. The teeth of the pinion were designed

to be perpendicular to the rack teeth. But the helical teeth replaced perpendicular ones since they reduce tooth pressure and to give some irreversibility [2]. The pinion is rotated by steering shaft which is controlled by steering wheel. The lateral moment in the rack caused by pinion teeth causes the displacement of tie rod which is connected to vehicle wheel. So the displacement of tie rod will steer the vehicle wheels accordingly. The stiffness of power assisted rack-and-pinion steering gear has been analyzed in [6]. A dynamic model of the steering system is derived in [7], where the authors classified the steering system into two subsystems which are mechanical and hydraulic systems.
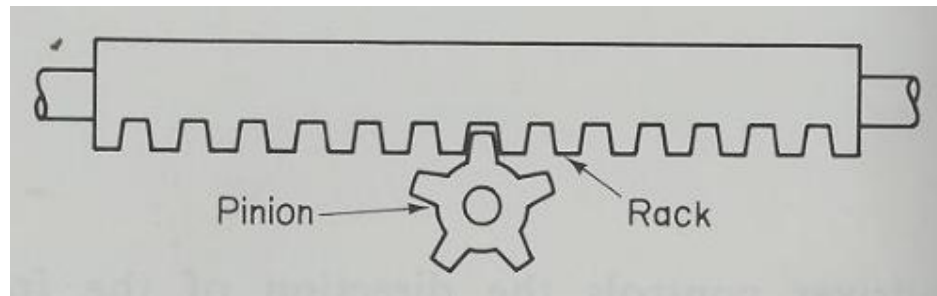
Figure 5: Rack-and-pinion gear [5]

Figure 6 is a photo of rack and pinion steering gear. In the photo we could observe the joint in which steering column fits in, in order to get contact with pinion. The pinion inside of the black rod displaces the rack which will displace the pitman arms that can be found on both ends of the photo.
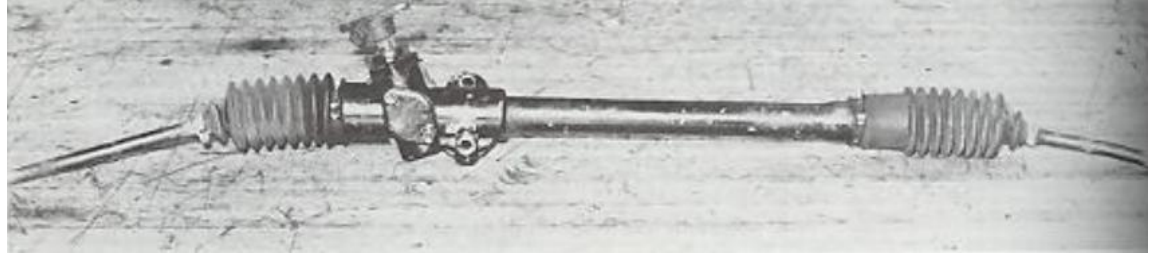
Figure 6: Photo of rack and pinion steering gear [5]

1.3 The Power Steering

A power steering is basically power-assisted standard steering [5]. A variety of causes can increase the static steering torque. The causes are low pressure tires, the radial tire, the tendency to front wheel drive, and consequent greater concentration of weight on the front part of the car [3]. The increased steering torque will make the driver feel very difficult to move the steering wheel. Therefore power steering has to be employed to reduce the steering torque exerted by the driver through the assist torque provided by external power source.

Power steering is mainly classified into two types according to the way they provide assist torque. The two types are hydraulic power steering (HPS) and electric power steering (commonly known as Electric power assist steering or EPAS).

HPS typically uses a servo valve arrangement which has two parallel throttle routes. One route is integrated into pinion shaft and the other one is out of the pinion

shaft. As the driver applies torque to steering wheel, the valve will monitor the flow of the hydraulic fluid into or out of the pinion shaft. The inflow or the outflow of the fluid will cause the lateral moment of the rack towards left or right, causing the moment in tie rod, finally assisting the driver steer the vehicle wheels. Here hydraulic pump is used to generate the external power to monitor the flow of the hydraulic fluid. Hydraulic pump is driven by the engine and connected to the engine with a belt.

EPAS uses an electric motor to generate the needed assist torque. Sensors detect the steering torque applied by the driver and provide input to the electric motor which will generate assist torque through which the actual torque applied by the driver is reduced. Hence the steering feeling of the driver will be improved.

EPAS has many advantages over traditional HPS. EPAS is more fuel efficient than continuously engine-driven HPS because it will not run electric motor unless the assist torque is needed. In addition, EPAS does not need as much space as HPS since the hydraulic pump and its setup can be removed.

1.4   The Control Issue

The control goal in the EPAS is to drive the electric motor to provide the assist torque so the steering feel of the drive is improved. Unexpected external disturbance (due to road conditions) and the uncertainty of system parameters make the controller design challenging. The other control problem found in power steering is dependability of assistance on the speed of the car.

1.4.1 Literature review

In [1], a PI controller is employed to minimize the difference between the reference torque, which is determined by a predefined torque map, and actual steering torque. A PD controller is introduced in [8, 9] to EPAS. In [10], an advanced opto-isolated torque sensor is used to sense the steering torque and a PID control algorithm is used to control the column-type electric power steering (EPS-TT). In [11] the EPS system is decoupled to two subsystems namely angle controlled and torque controlled systems and a PID controller is applied to both systems. A Fuzzy Neural Network PID control is designed for EPAS in [12]. The researchers in [13] have concentrated on detecting the measurement faults of sensors and isolating the faults from sensors to guarantee the reliability and safety of EPS system. A Fault detection and Isolation algorithm is proposed in [13] and is composed by two step process. The parity equation which detects the faults of the phase current sensor and the faults of the angular velocity sensor is developed in one of the steps. In the other step, an assist steering torque is determined by comparing it with threshold valves [13]. In [14], a lead lag compensator is applied to ensure the stability of EPAS and better steering feel. The development of a novel method using a constrained optimization control can be found in [15] where the steering feel issues are addressed. In [16] a dynamic model of the EPAS is derived and the stability of the system is analyzed. An H_∞ method is applied to EPAS system in [17], which has also addressed robustness and stability issues of the EPAS. In [18] a two-controller structure has been proposed for the EPAS that is divided into two subsystems namely motor torque and steering motion systems. Motor torque subsystem is for producing assist torque for

which a H_2 controller is applied. Steering motion subsystem is for improving the driver's driving feel for which a H_∞ controller is applied. In [19], a steering characteristic curve was designed and analyzed to calculate the reference torque. In [19], a PID algorithm based on the calculated reference torque is employed to the EPAS to get better performance than advanced controllers. A steer-by-wire control system is presented in [20], where two embedded electronic control modules were designed for articulated vehicles. In [20], one electronic module will take over the control if it detects the fault in the other module. The control modules will warn the operator in case of any system failures. The authors in [21] performed a kinematics and sensitivity optimization for rack-and-pinion steering system and came up with different types of linkage (variation in link lengths) to choose with as per requirement. The steering wheel returnability at different conditions such as low speed, maximum speed, maximum steering angle etc is studied in [22]. A suspension model and tire model have been developed in [22] as well. In [23] the lag in response during rapid steering in hydraulic power steering system is analyzed. The study on steering-wheel grip force of both male and female drivers is performed in [24]. A H_∞ robust control design has been proposed for EPAS in [25]. In [26], a compound controller of Cerebellum Model Articulation Controller (CMAC) and PID are proposed for the EPAS. In this paper, the feedback control is realized by PID to make system stable while feed forward controller is neural network based CMAC which is used to increase the system responding speed and control precision. A low pass filter based automotive electric power steering controller is analyzed in [27]. In [28], the EPAS's working principle is introduced and the effect of control theory on the EPAS is explained with case studies.

The advanced controllers reported in current literature [17, 18, 20 and 25] have multiple tuning parameters and complicated mathematical structures, which make them difficult to implement in the real world. The PID controllers and lead-lag compensators [8, 9, 10, 11, 12 and 14] for the EPAS system are not robust against disturbances and parameter variations. Therefore, an easy-to-implement and robust controller is desired for the EPAS system.

1.4.2 Thesis contribution

In this thesis, an active disturbance rejection controller (ADRC) is originally and successfully applied to the EPAS. The ADRC is very powerful in disturbance rejection and in being robust against parameter variations. Since EPAS is a 4th order plant (the details of system modeling will be introduced in Chapter II), a 5th order ADRC is used (the details of controller design will be explained in Chapter III). The transfer function representation of the ADRC controlled EPAS system has been developed. Frequency-domain analyses are conducted to verify the stability and robustness of the controller. The performance of the ADRC is also investigated through evaluating the steady-state error of the control system. ADRC only has two tuning parameters which make is simple to implement in the real world. In the thesis, the ADRC is simulated on a column-type EPAS. The simulation results verify the effectiveness of the controller.

1.5 Thesis outline

The following part of the thesis is organized as follows. Chapter 2 introduces dynamic modeling of the EPAS and control problem formulation. In this chapter, the differential equation modeling, state space modeling, and block diagrams of the plant (EPAS) will be given. Chapter 3 introduces the development of the ADRC on the EPAS. Chapter 4 conducts the frequency response analysis. Simulation results are shown in Chapter 5. The concluding remarks and future research are given in Chapter 6.

CHAPTER II

MODELING OF EPAS SYSTEM

This chapter talks about the dynamic modeling of a column-type EPAS system. The differential equation modeling, state-space model, and transfer function representation of the EPAS system will be developed in this chapter

2.1 Dynamic modeling of EPAS system

The power steering system includes steering column, steering rack, torque sensor, and power assist motor with gear box [12]. The mechanical model of the power steering system is shown in Figure 7 which is obtained from [13].
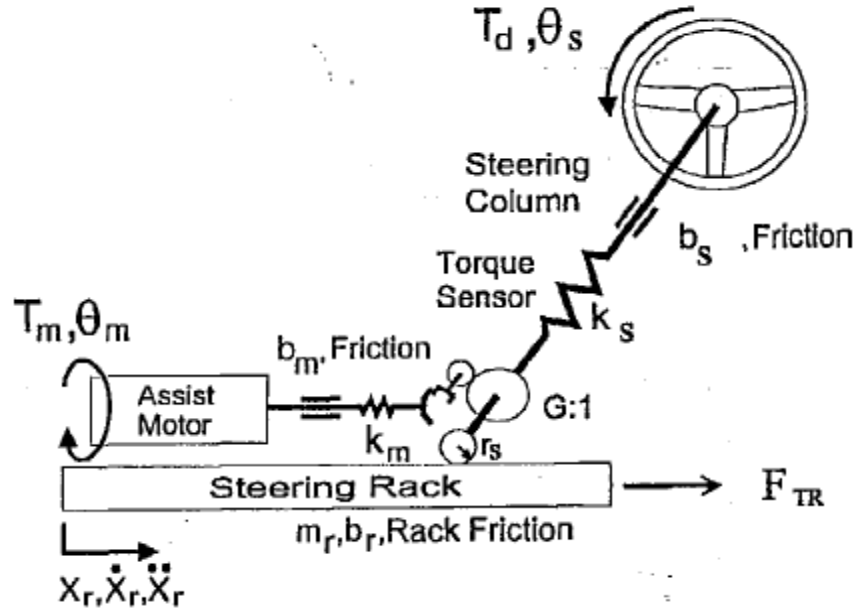
Figure 7 Dynamic model of EPAS [13]

The governing equations of the dynamic motion of the EPAS system under assumption of relatively high assist stiffness are obtained from [12] and given by

$$J_s \ddot{\theta}_s + b_s \dot{\theta}_s + K_s \theta_s = T_d + \frac{K_s}{R_s} x \tag{1}$$

$$m_e \ddot{x} + b_e \dot{x} + K_e x = \frac{T_a G}{R_m} + \frac{K_s}{R_s} \theta_s + F_\delta \tag{2}$$

$$y = K_s \left(\theta_s - \frac{x}{R_s} \right) + v_t \tag{3}$$

$$T_a = \frac{K_a}{G} (K_s (\theta_s - \frac{x}{R_s}) + v_t), \, 0 \le K_a \le K_a^{max} \tag{4}$$

Equation (1) gives the dynamics relating the angle of rotation (θ_s) with the driver torque (T_d) and the displacement of rack(x). Equation (2) represents the dynamics of the displacement of rack(x) and assist torque (T_a). Equations (3) and (4) show relationship

14

between the measured output (y) and assist torque (T_a). In (1), (2) (3) and (4), J_s, θ_s, K_s, b_s are moment of inertia, angle of rotation, stiffness coefficient and damping ratio, respectively, of steering column, R_s , R_m are column and rack pinion radii, m_e, x, K_e, b_e are effective rack mass, displacement of rack from equilibrium position, stiffness coefficient of rack and damping coefficient of rack respectively [11], G is gear ratio, T_d is driver torque, T_a is assist torque, F_δ is disturbance force from road, and v_t is measurement noise [12].

Figure 8 shows the torque flow of the steering system. The driver's torque (T_d) actuates the motor which sends the assist torque to displace the rack. Output y is the actual torque acting on the rack to displace it which should be identical to driver torque.

T_d → Steering Column → Motor → T_a → Rack → y
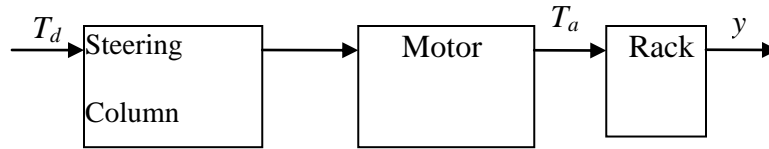
Figure 8 Torque flow of EPAS

Applying Laplace transform to equations 1-4, we can derive the transfer function between output(y) and input (T_d). The plant transfer functions are obtained from [12, 13] and repeated as follows.

$$S(s) = K_a P_c(s) G(s)$$

$$G(s) = \frac{K_s (J_s s^2 + b_s s)}{R_s^2 (A_c(s))}$$

$$A_c(s) = d_s d_x - \frac{K_s}{R_s^2} \tag{5}$$

$$d_s = J_s s^2 + b_s s + K_s, \, d_x = m_e s^2 + b_e s + K_e$$

$$P_c(s) = \frac{p_t}{s + p_t} \frac{p_a}{s + p_a}$$

In (5), p_t, p_a are specified bandwidths of torque sensor and electric actuator respectively. K_a is the assist torque, d_s is dynamics of steering column, d_x is dynamics of rack and $P_c(s)$ represents dynamics of sensor and actuator.

The essence of an EPAS system is an electronically controlled assist motor that can be taken as a smart actuator. The EPAS is a classical example of the actuator operating under feedback control. When an appropriate assist torque from the assist motor is applied in the same direction as the driver's steering direction, the amount of steering torque required by the driver for steering can be considerably relieved. From (5), the transfer function representation of the EPAS system can be illustrated by Figure 9 where K_a represents assist gain, $D(s)$ is controller, v_t is noise signal. F_δ is external disturbance.
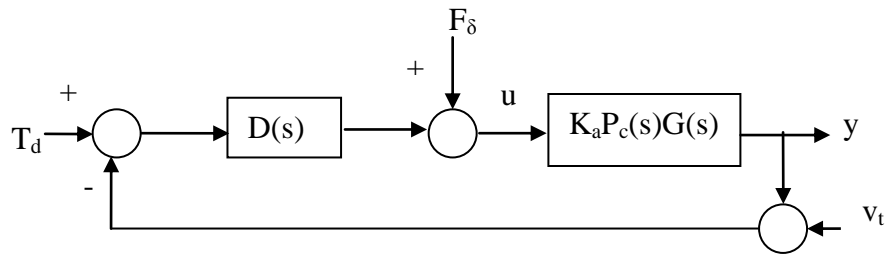
Figure 9: Unity feedback system for EPAS

16

As mentioned earlier, our control goal is to make the output torque y follow the driver's input torque T_d at any given situations such as parking condition (worst case) or high-speed condition. The driver's input torque (T_d) is supposed to turn the steering wheels in order to steer the vehicle in required direction.

2.2 State space modeling of EPAS system

Substituting the $G(s)$ and $P_c(s)$ in (5) into $S(s)$ yields

$$S(s) = \frac{y(s)}{u(s) + F_\delta(s)} = K_a \frac{p_a}{s + p_a} \frac{p_t}{s + p_t} \frac{K_s(J_s s^2 + b_s s)}{R_s^2((J_s s^2 + b_s s + K_s)(m_e s^2 + b_e s + K_e) - \frac{K_s}{R_s^2})}$$

(6)

Equation (6) can be rewritten as

$$\frac{y(s)}{u(s) + F_\delta(s)} = \frac{a_2 s^2 + a_1 s}{b_6 s^6 + b_5 s^5 + b_4 s^4 + b_3 s^3 + b_2 s^2 + b_1 s + b_0}$$

(7)

where the parameters a_i and b_i are the coefficients of the numerator and denominator of the transfer function (7). The coefficients can be obtained through comparing the right sides of equations (6) and (7).Cross multiplying both sides of (7) and converting it into ODE yields

$$y^{(6)} + a_1 y^{(5)} + a_2 y^{(4)} + a_3 \dddot{y} + a_4 \ddot{y} + a_5 \dot{y} + a_6 y = b_1 \ddot{u} + b_2 \dot{u}$$

(8)

17

Integrating the plant (8) twice produces

$$y^{(4)} + a_1 \ddddot{y} + a_2 \dddot{y} + a_3 \dot{y} + a_4 y + a_5 \int y + a_6 \iint y = b_1 u + b_2 \int u \qquad (9)$$

This plant could be rewritten in the form of

$$y^{(4)} = f(\dddot{y}, \ddot{y}, \dot{y}, y, \int y, \iint y, \int u, w) + b_1 u \qquad (10)$$

where "f" is the generalized disturbance that represents all internal and external disturbances and ω denotes external disturbance and measurement noise, and b_1 represents controller gain.

One of the objectives of representing the plant in the form of (10) is to observe and estimate the generalized disturbance term (f) and cancel it out so that the system could be controlled by a simple PD controller. Since the EPAS plant can be represented by a 4th order plant (10), a fifth-order ESO has to be designed [29]. The ESO will be used to observe/estimate both internal states of the plant, and the generalized disturbance f.

We choose the first state variable y_1 as y. The other four state variables are chosen as y_2 ($y_2 = \dot{y}$), y_3 ($y_3 = \ddot{y}$), y_4 ($y_4 = \dddot{y}$), and y_5 ($y_5 = f$). We suppose f is differentiable, and the derivative of f is bounded.

Then the ODE model (10) of the EPAS system can be represented by

$$
\begin{aligned}
\dot{y}_1 &= y_2 \\
\dot{y}_2 &= y_3 \\
\dot{y}_3 &= y_4 \\
\dot{y}_4 &= y_5 + bu \\
\dot{y}_5 &= \dot{f} = h
\end{aligned}
\qquad (11)
$$

The matrix form of (11) is represented by (12)

$$
\begin{bmatrix} \dot{y}_1 \\ \dot{y}_2 \\ \dot{y}_3 \\ \dot{y}_4 \\ \dot{y}_5 \end{bmatrix} = \begin{bmatrix} 0 & 1 & 0 & 0 & 0 \\ 0 & 0 & 1 & 0 & 0 \\ 0 & 0 & 0 & 1 & 0 \\ 0 & 0 & 0 & 0 & 1 \\ 0 & 0 & 0 & 0 & 0 \end{bmatrix} \begin{bmatrix} y_1 \\ y_2 \\ y_3 \\ y_4 \\ y_5 \end{bmatrix} + \begin{bmatrix} 0 \\ 0 \\ 0 \\ b \\ 0 \end{bmatrix} u + \begin{bmatrix} 0 \\ 0 \\ 0 \\ 0 \\ 1 \end{bmatrix} h
$$

(12)

In (12), b is control gain which is approximately equal to b_1.

So far we have obtained the state-space model of the EPAS system. The model represented by (12) will be used for controller design. In the next chapter, we will develop an active disturbance controller (ADRC) based on (12) for the EPAS system.

CHAPTER III

CONTROLLER DESIGN FOR AN EPAS SYSTEM

In this chapter, the working principle of ADRC and extended state observer (ESO) will be introduced. The application of the ADRC to the EPAS system will be developed.

3.1 The introduction of ADRC and ESO

ADRC used the concept of PID in classical control theory and the observer concept in modern control theory to drive the system output to a desired signal. It proves to be the capable replacement of PID with remarkable advantages in performance and practicality [29].

The name of the ADRC suggests that it reject external disturbance actively. When it comes to the external disturbance, it could be input or output disturbance, sensor noise, structural uncertainty in system parameters, or any other kind of unwanted signal. To summarize, the disturbance can be generalized as the difference between a mathematical model of a plant and the actual plant. We can also say the generalized disturbance represents any other inputs of the system excluding the control input.

The basic idea of ADRC is to observe an extra state, which is the generalized disturbance, observe the state and any other internal states of the plant, and eventually design the control law based on the observed states.

3.2 Application of the ADRC to EPAS system

A significant amount of research work has been reported on application of ADRC to all type of plants [29-35], where ADRC is mainly developed on 2nd order plants for which a third-order ESO is designed. In our case as the EPAS system is a 4th order system (as given in (10)) we should use a higher-order ESO to observe the extra state.

Based on (12) the ESO is designed as

$$\dot{Z} = AZ + Bu + L(y - \hat{y})$$
$$\hat{y} = CZ$$

$$(13)$$

Where Z is estimated state vector and $\hat{y}$ is observed output,

$$A = \begin{bmatrix} 0 & 1 & 0 & 0 & 0 \\ 0 & 0 & 1 & 0 & 0 \\ 0 & 0 & 0 & 1 & 0 \\ 0 & 0 & 0 & 0 & 1 \\ 0 & 0 & 0 & 0 & 0 \end{bmatrix}, \; B = \begin{bmatrix} 0 \\ 0 \\ 0 \\ b \\ 0 \end{bmatrix}, \; \text{and } C = \begin{bmatrix} 1 & 0 & 0 & 0 & 0 \end{bmatrix} \qquad (14)$$

The characteristic equation for (13) and (14) is denoted by $\lambda(s)$ $= |sI - (A - LC)| = s^5 + l_1 s^4 + l_2 s^3 + l_3 s^2 + l_4 s + l_5$. The observer gains are chosen as

$$\begin{aligned} l_1 &= 5\omega_0 \\ l_2 &= 10\omega_0^2 \\ l_3 &= 10\omega_0^3 \\ l_4 &= 5\omega_0^4 \\ l_5 &= \omega_0^5 \end{aligned} \qquad (15)$$

where ω_o is the bandwidth of observer. By choosing the observer gains as (15), we our characteristic equation can be rewritten as $\lambda(s) = (s + \omega_0)^5$.

The control signal is chosen as

$$u = \frac{u_0 - z_5}{b} \qquad (16)$$

where z_5 is observed generalized disturbance which is approximately equal to f.

Substituting (16) into (10) yields

$$y^{(4)} = f(\ddddot{y}, \dddot{y}, \dot{y}, y, \int y, \int y, \int u, w) + b_1(\frac{u_0 - z_5}{b}) \qquad (17)$$

Let $b = b_1$ and suppose ESO estimates f accurately. Then the resulting equation from (17) will be

$$y^{(4)} = f + u_0 - z_5 \tag{18}$$

Since $f \approx z_5$,

$$y^{(4)} \cong u_0, \tag{19}$$

Equation (19) can easily be controlled by a proportional derivative controller as follows. In (20), r is a reference signal and $z_1,\ z_2,\ z_3, z_4$ are observed states.

$$u_0 = K_p(r - z_1) + K_d(\dot{r} - z_2) + K_{dd}(\ddot{r} - z_3) + K_{ddd}(\dddot{r} - z_4) \tag{20}$$

In (20), we choose the controller gains as $K_p = w_c^4$, $K_d = 4w_c^3$, $K_{dd} = 6w_c^2$, $K_{ddd} = 4w_c$ and $w_o = 5w_c$. So the only tuning parameter of the controller will be reduced to ω_c. The details about how to tune the controller and observer parameters ω_c and ω_o can be found in [32].

3.3 Transfer function representation of ADRC controlled EPAS

The Laplace transform of the ESO (13) is

$$sZ(s) = (A - LC)Z(s) + Bu(s) + Ly(s) \tag{21}$$

where $Z(s)$ is the Laplace transform of the estimated state vector. Then $Z(s) = \hat{X}(s)$. Substituting (20) into (16), we will have the Laplace transform of the controller as follows.

23

$$u(s) = \frac{1}{b}\begin{bmatrix} K_p & K_d & K_{dd} & K_{ddd} & 1 \end{bmatrix} \begin{bmatrix} r(s) \\ sr(s) \\ s^2 r(s) \\ s^3 r(s) \\ s^4 r(s) \end{bmatrix} - \frac{1}{b}\begin{bmatrix} K_p & K_d & K_{dd} & K_{ddd} & 1 \end{bmatrix} Z(s)$$

(22)

Substituting (22) into (21) yields

$$u(s) = \frac{1}{b} \frac{s^5 + l_1 s^4 + l_2 s^3 + l_3 s^2 + l_4 s + l_5}{s^5 + \beta_1 s^4 + \beta_2 s^3 + \beta_3 s^2 + \beta_4 s}(K_p + K_d s + K_{dd} s^2 + K_{ddd} s^3 + s^4) r(s)$$

$$- \frac{1}{b} \frac{\mu_1 s^4 + \mu_2 s^3 + \mu_3 s^2 + \mu_4 s + \mu_5}{s^5 + \beta_1 s^4 + \beta_2 s^3 + \beta_3 s^2 + \beta_4 s} y(s)$$

(23)

where,

$$\mu_1 = l_1 K_p + l_2 K_d + l_3 K_{dd} + l_4 K_{ddd} + l_5$$
$$\mu_2 = l_2 K_p + l_3 K_d + l_4 K_{dd} + l_5 K_{ddd}$$
$$\mu_3 = l_3 K_p + l_4 K_d + l_5 K_{dd}$$
$$\mu_4 = l_4 K_p + l_5 K_d$$
$$\mu_5 = l_5 K_p$$
$$\beta_1 = K_{ddd} + l_1$$
$$\beta_2 = K_{dd} + K_{ddd} l_1 + l_2$$
$$\beta_3 = K_d + K_{dd} l_1 + K_{ddd} l_2 + l_3$$
$$\beta_4 = K_p + K_d l_1 + K_{dd} l_2 + K_{ddd} l_3 + l_4$$

Let

$$G_c(s) = \frac{\mu_1 s^4 + \mu_2 s^3 + \mu_3 s^2 + \mu_4 s + \mu_5}{b(s^5 + \beta_1 s^4 + \beta_2 s^2 + \beta_3 s^3 + \beta_4 s)}$$

$$H(s) = \frac{(s^5 + l_1 s^4 + l_2 s^3 + l_3 s^2 + l_4 s + l_5)(K_p + K_d s + K_{dd} s^2 + K_{ddd} s^3 + s^4)}{\mu_1 s^4 + \mu_2 s^3 + \mu_3 s^2 + \mu_4 s + \mu_5}$$

(24)

Then (23) could be written as

$$u(s) = H(s)G_c(s)r(s) - G_c(s)y(s)$$

(25)

From (25), the closed loop control system can be represented by Figure 10, where $F_d(s)$ is an external disturbance function.
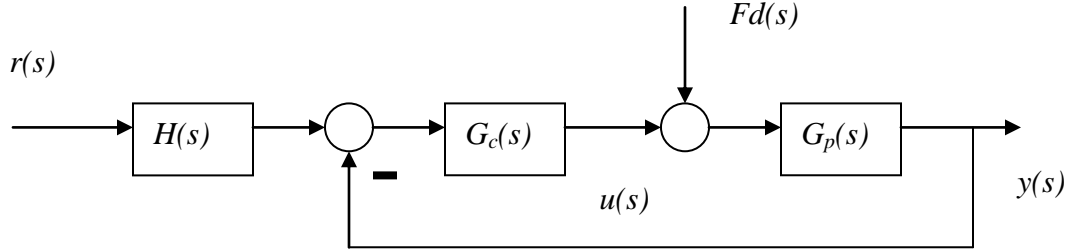

Figure 10: The block diagram of a closed-loop ADRC control system

In Figure 10, $G_p(s)$ is the transfer function of the EPAS plant (as given by (6)).

From Figure 10, open-loop transfer function $G_o(s)$ is

$$G_o(s) = G_c(s)G_p(s)$$

(26)

And closed loop transfer function $G_{cl}(s)$ is

$$G_{cl}(s) = \frac{y(s)}{r(s)} = \frac{H(s)G_c(s)G_p(s)}{1 + G_c(s)G_p(s)}$$

(27)

25

The transfer function from disturbance input to output is denoted by $G_d(s)$ and

$$G_d(s) = \frac{y(s)}{D(s)} = \frac{G_p(s)}{1 + G_c(s)G_p(s)} \qquad (28)$$

CHAPTER IV

FREQUENCY RESPONSE ANALYSIS

In this chapter, frequency-domain analyses are conducted to investigate the stability and robustness of the controller. In addition, the tracking performance of the ADRC is also tested through evaluating the steady-state error of the control system.

4.1 Steady state error

The mathematical representation of the EPAS is given by (6). The system parameters are given in Appendix. Substituting the system parameters into (6) yields

$$\frac{y}{u+F_d} = \frac{817203.2444s^2 + 7354829.19970s}{0.0011s^6 + 0.9937s^5 + 229674s^4 + 907915s^3 + 995453 \times 10^4 s^2 + 3589177 \times 10^5 s + 2.276 \times 10^8}$$

(29)

In order to avoid the differentiator block in Simulink, we integrate the plant twice and the resulting plant in Simulink model can be found in appendix.

Figure 11 shows the external disturbance that is applied to ADRC controlled EPAS system.
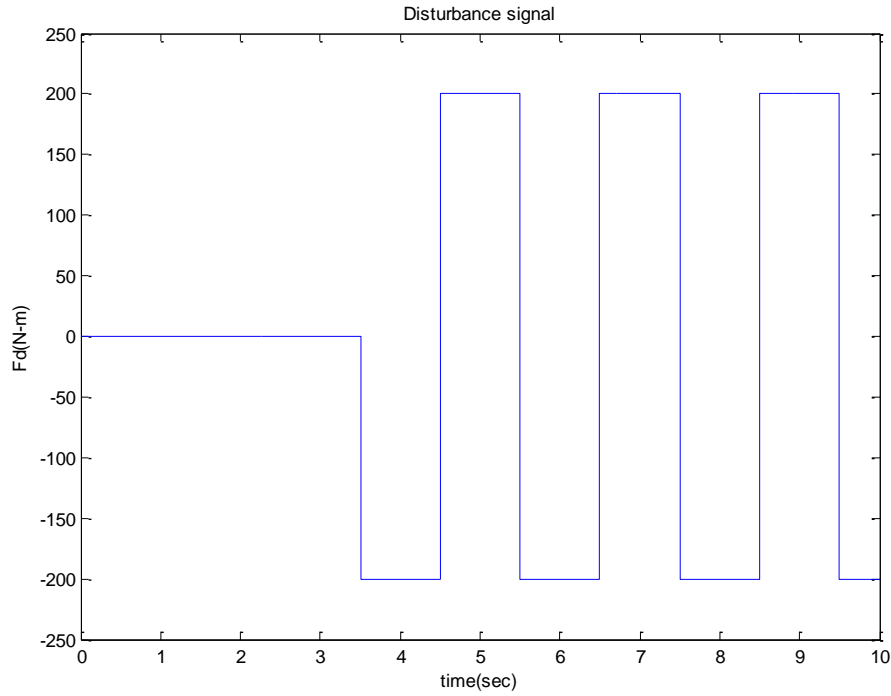

Figure 11: External disturbance signal

We suppose the reference signal *r(s)* is desired torque. Our goal is to make the torque output of the EPAS system to follow the desired torque. From [11], the reference signal is a sine wave for the EPAS system. The expression for *R(s)* is given by

$$r(s) = 5\sin(0.25t) \tag{30}$$

In (20), the magnitude of the reference torque is 5 *Nm*, and the angular frequency of it is 0.25 *rad/s*. The reference signal is shown in Figure 12.
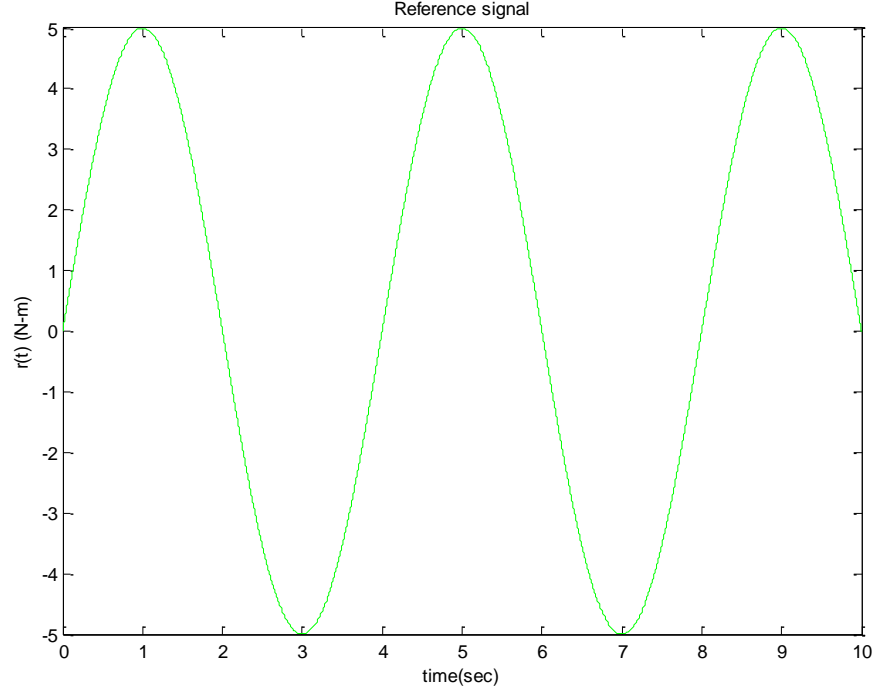

Figure 12: Reference signal

From the closed loop transfer function (27), the steady-state output of EPAS system is

$$x_{ss} = A|G_{cl}(j\omega)|\sin(\omega t + \phi)$$

(31)

where $|G_{cl}(j\omega)|$ is the magnitude of the transfer function and the phase shift is

$$\phi = \angle G_{cl}(j\omega) = \tan^{-1}\frac{\text{Im}(G_{cl}(j\omega))}{\text{Re}(G_{cl}(j\omega))}$$

(32)

Define the magnitude error between steady state output and reference signal as e_m, which is represented by

$$e_m = A - A|G_{cl}(j\omega)| \tag{33}$$

The magnitude error and phase shift versus the controller gain (or controller bandwidth) ω_c are shown in Figure 13, where both magnitude error and phase shift of stead-state output of the ADRC controlled EPAS system are converging to zeroes with the increase of the controller bandwidth[36].
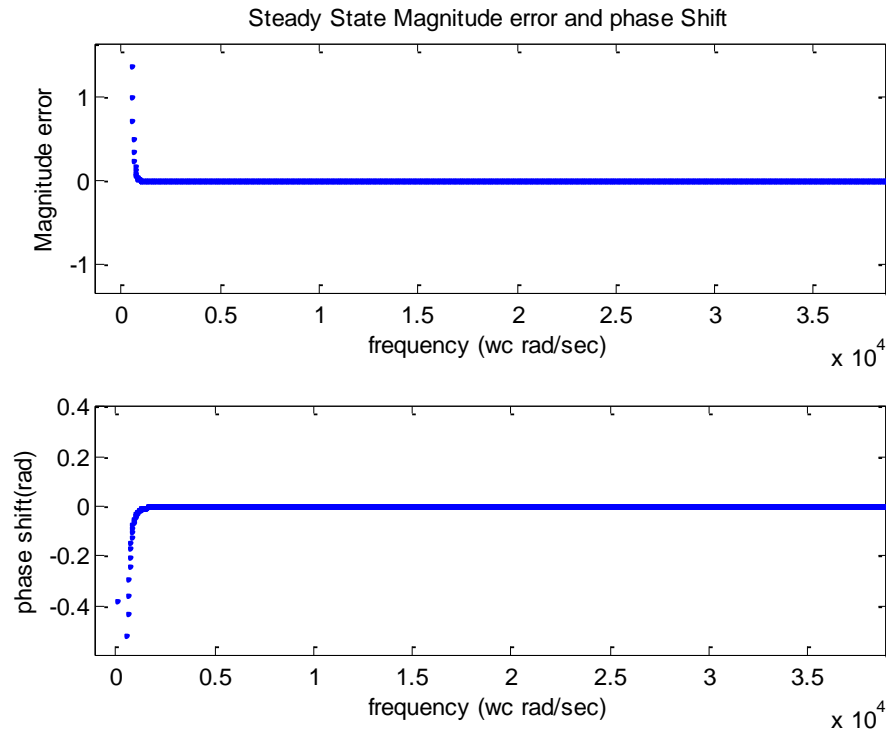

Figure 13: The magnitude error and phase shift of the steady-state output of the ADRC controlled EPAS system

4.2 Loop Gain Frequency Response

The bode plots of loop-gain transfer function (26) are shown in Figure 14 where $\omega_c = 5*10^3$ rad/sec, and assist gain Ka is ranging from 1 to 40 (K_a=40 is the worst condition since it represents parking mode where lot of assistance for steering the wheel is required than that of driving mode). From this figure, we can see that despite the change in the assist gain (Ka) that also reflects the change in the speed of the automobile (it may be in parking mode (Ka=40) or at high speed (Ka=1)), there are no changes in the Bode plots of the system. So the system is robust against the variations of Ka.
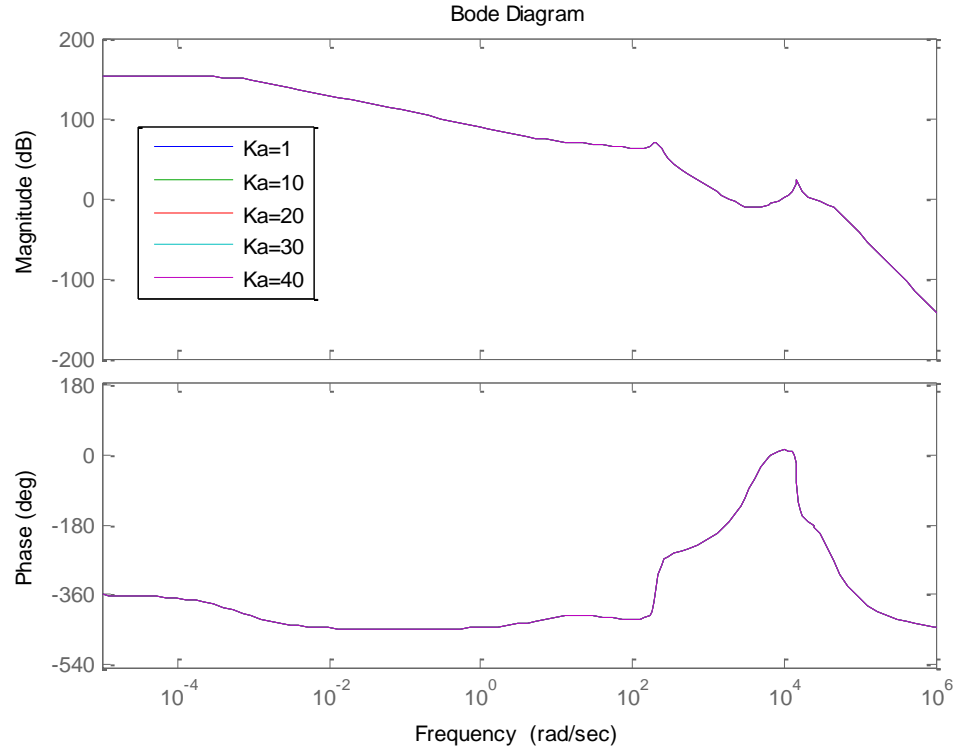

Figure 14: Bode plots of loop gain transfer function with changing assist gain (Ka)

4.3 External Disturbance Rejection

Figure 15 shows the Bode diagrams of the transfer function between disturbance input and torque output in the presences of system parameter variations (from 0% through 20%). From the figure, we can see that the disturbance can be rejected by the ADRC controller even in the presences of parameter variations.
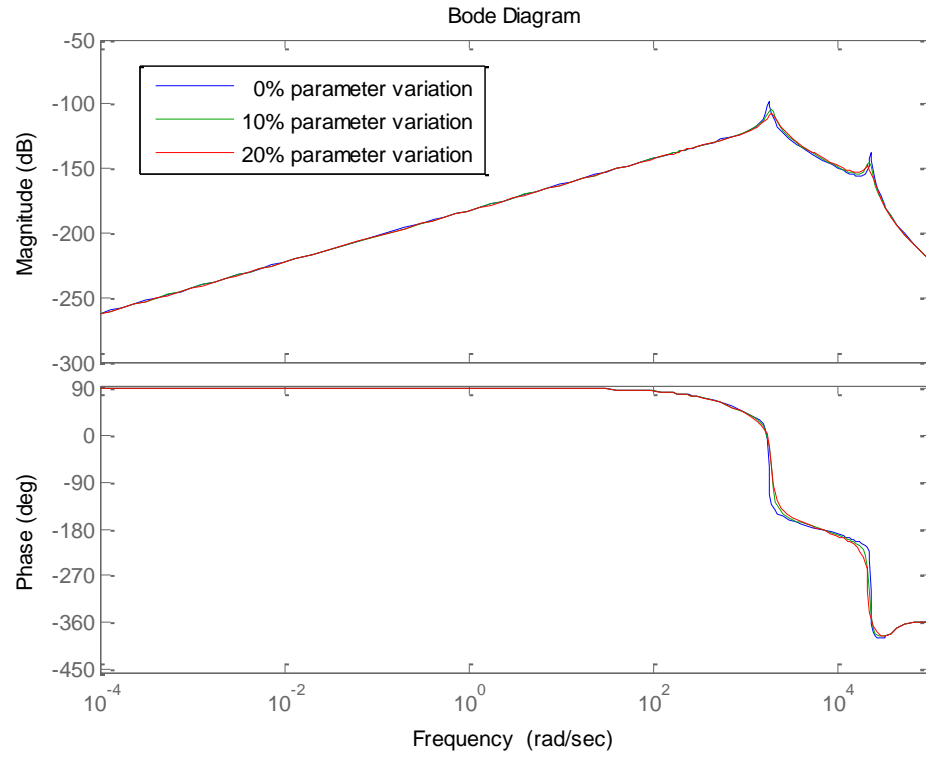

Figure 15: Bode plots of $G_d(s)$ with parameter variations

4.4 Robustness and Stability Margins

The Bode diagrams of loop gain transfer function ($G_o(s)$) with varying system parameters ($J_s, b_s, K_s, R_s, m, J_m, R_m, b_m, b$) as ω_c=5000 rad/s are shown in Figure 16. The stability margins of the system with variant system parameters as ω_c=5000 rad/s are listed in Table 1.

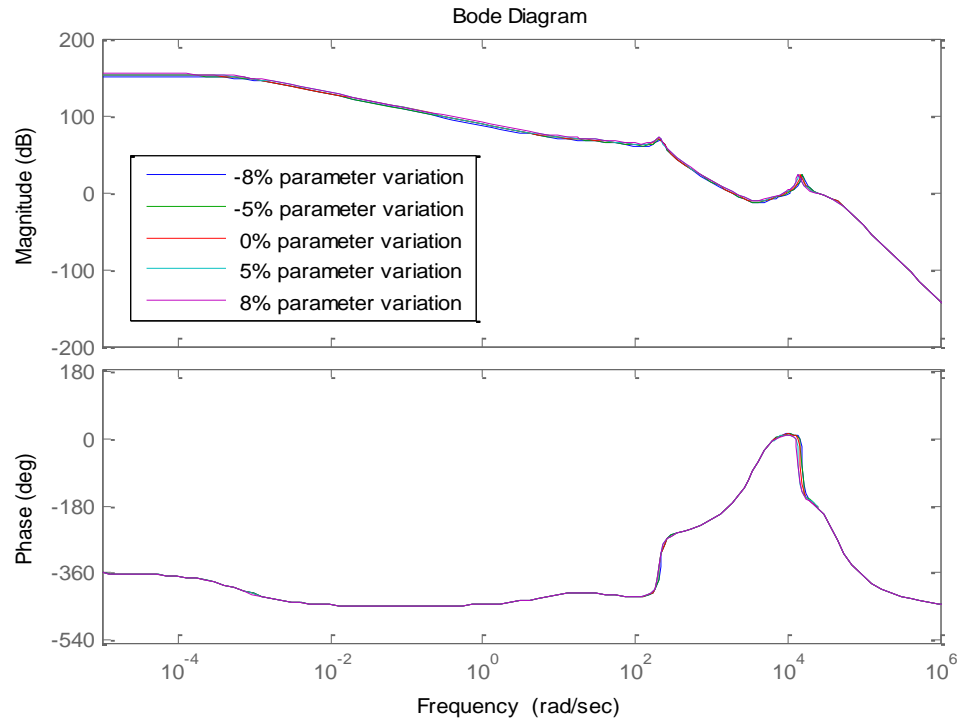Figure 16: Bode plot of loop gain transfer function with parameter variation as

ω_c=5000 rad/s

Table 1: Gain and phase margins of the ADRC controlled EPAS system as

w_c=5000 rad/s

Parameter variations	Gain Margin(dB)	Phase Margin(deg)
-8% variation	0.98	0.65
-5% variation	1.008	0.08
0% variation	1.06	2.16
5% variation	1.10	3.26
8% variation	1.12	4.92

From Figure 16 and Table I, we can see that with the change in the parameters, system have positive stability margins and minimal change in margins. This proves that the system is stable and robust against changes of parameters.

The Bode diagrams of loop gain transfer function ($G_o(s)$) with varying system parameters ($J_s, b_s, K_s, R_s, m, J_m, R_m, b_m, b$) as ω_c=8000 *rad/s* are shown in Figure 17. The stability margins of the system with variant system parameters as ω_c=8000 *rad/s* are given in Table II.
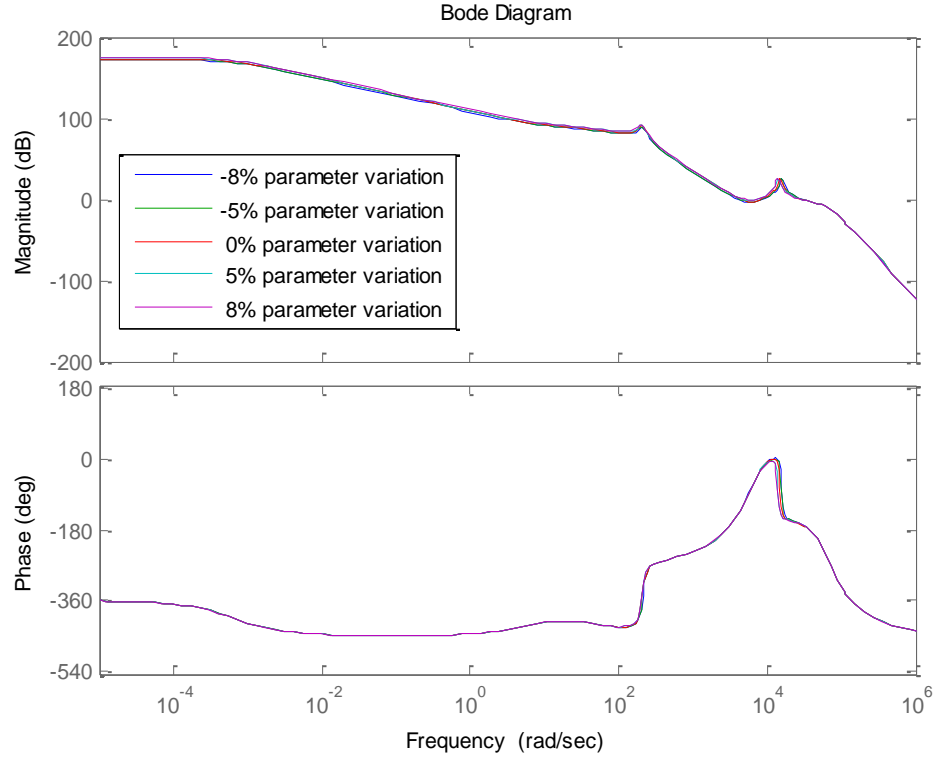
Figure 17: Bode plot of loop gain transfer function with parameter variations as

ω_c=8000 *rad/s*

Table 2: Gain and phase margins of the ADRC controlled EPAS system with

ω_c=8000 *rad/s*

Change in parameters	Gain Margin(dB)	Phase Margin(deg)
-8% variation	1.37	12.9435
-5% variation	1.3861	13.4772
0% variation	1.4097	14.2556

5% variation	1.4299	14.9178
8% variation	1.4407	15.2683

From the Figure17 and Table 2, we can see that the stability of the system are better than that of the system with w_c=5000 *rad/s*. Despite the change in the parameters, the control system has positive stability margins and minimal change in margins. This proves that the system is stable and robust for change of parameters.

CHAPTER V

SIMULATION RESULTS

In this chapter, the ADRC controller is simulated on the EPAS system, whose parameter values are given in Appendix. The simulation results will be used to test the effectiveness of the ADRC.

5.1 Tracking Performance

In this chapter, the controller bandwidth ω_c is chosen as 5000 rad/s and 8000 rad/s respectively. Accordingly the observer bandwidth ($\omega_{o=}5\omega_c$) is chosen as 25,000

rad/s and 40,000 *rad/s* respectively. The Simulink models, which were constructed to produce the simulation results, are provided in Appendix.

Figure 18 shows the reference signal *r(t)* which is a sine wave with amplitude 5*Nm* and frequency of 0.25 *rad/sec*. Our control goal is to control the EPAS to output a torque which is tracking the reference signal in the presences of disturbance and parameter variations. Figure 19 shows the external disturbance signal to be added to the control system. The magnitude of the disturbance signal is 200*Nm*, and frequency of it is 0.5 *rad/s*.
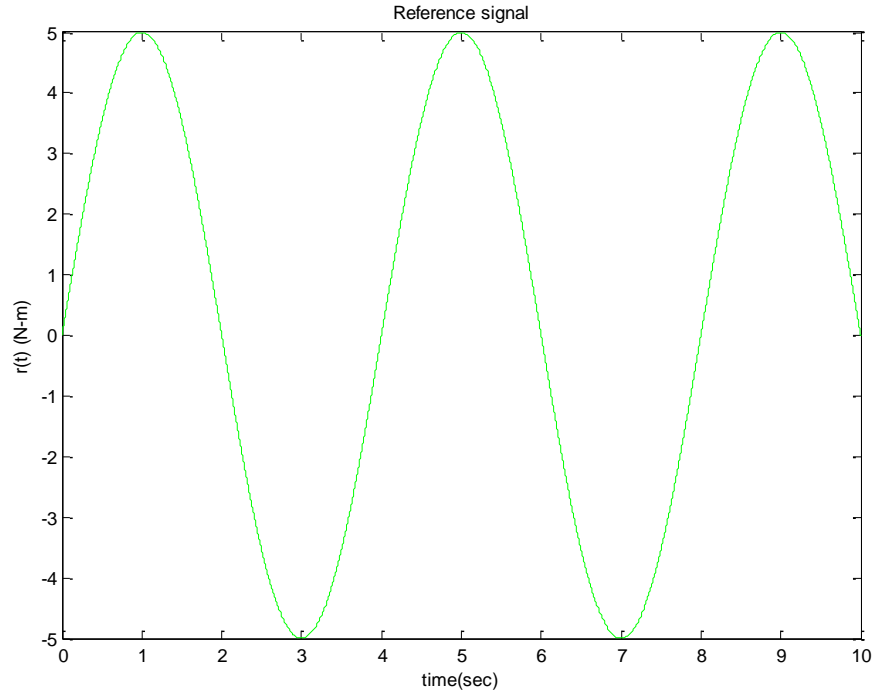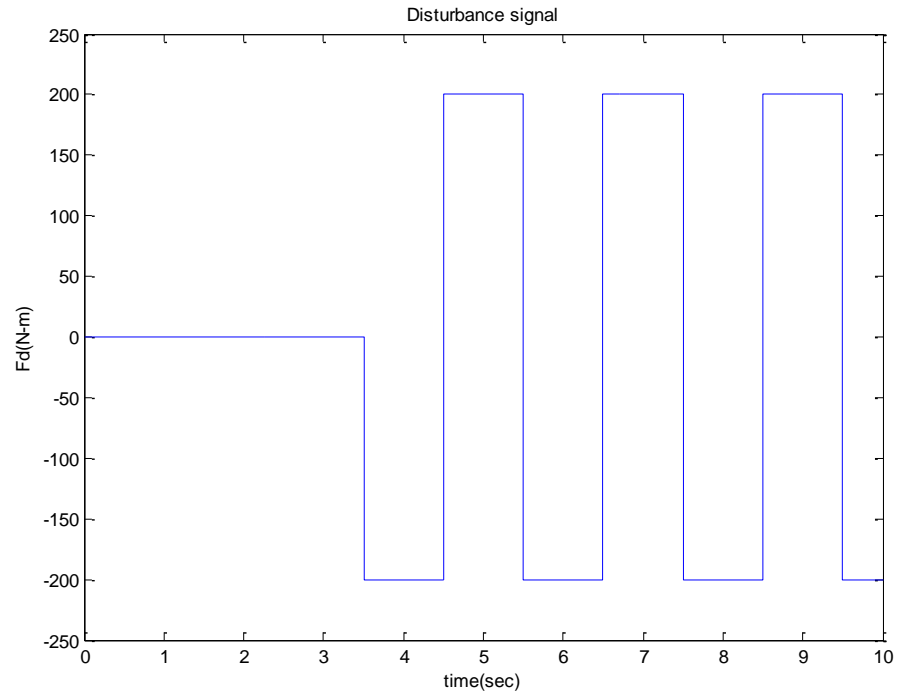

Figure 18: Reference signal (*r(t)*)

Figure 19: External disturbance signal with amplitude of 200N-m and angular frequency

of 0.5 rad/sec

Figure 20 and Figure 23 show the output signals of the ADRC controlled EPAS as *Ka* equals 1 and 40 respectively.
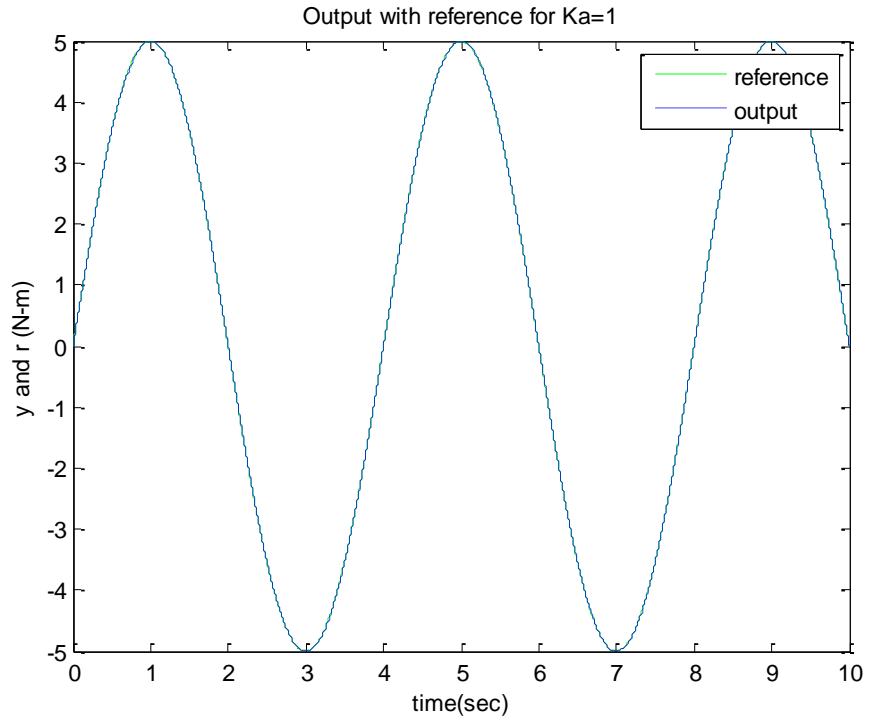
Figure 20: Output signal as *Ka*=1

From Figure 20, we can see that the output is following the reference signal very well. Figure 21 demonstrates that the disturbance at 8.5 second (the amplitude of disturbance is changing from -200Nm to 200Nm) has no effects on system output.
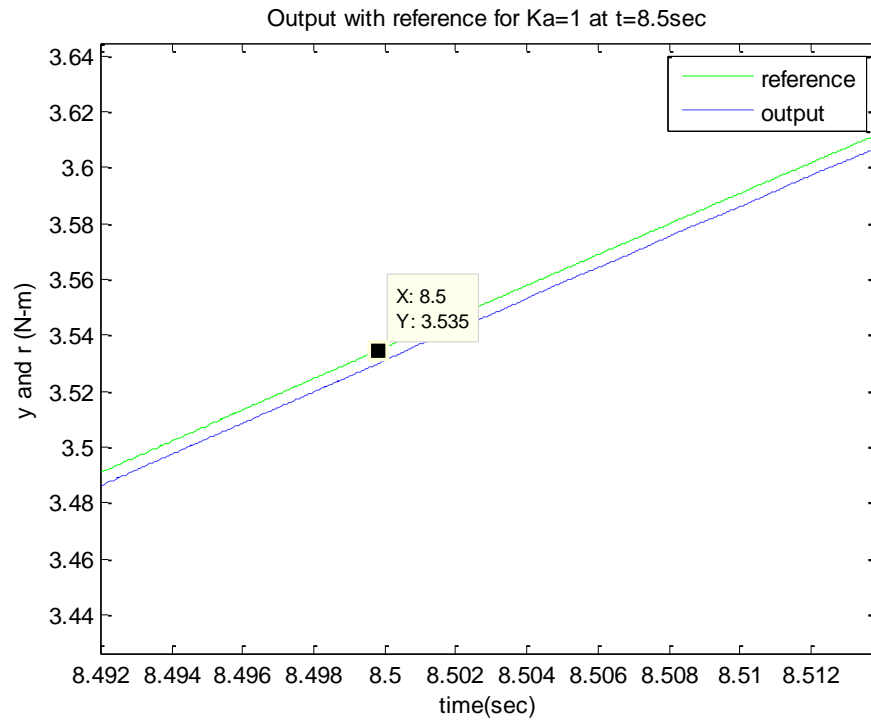
X: 8.5
Y: 3.535

Figure 21: Output signal at 8.5 sec as *Ka*=1
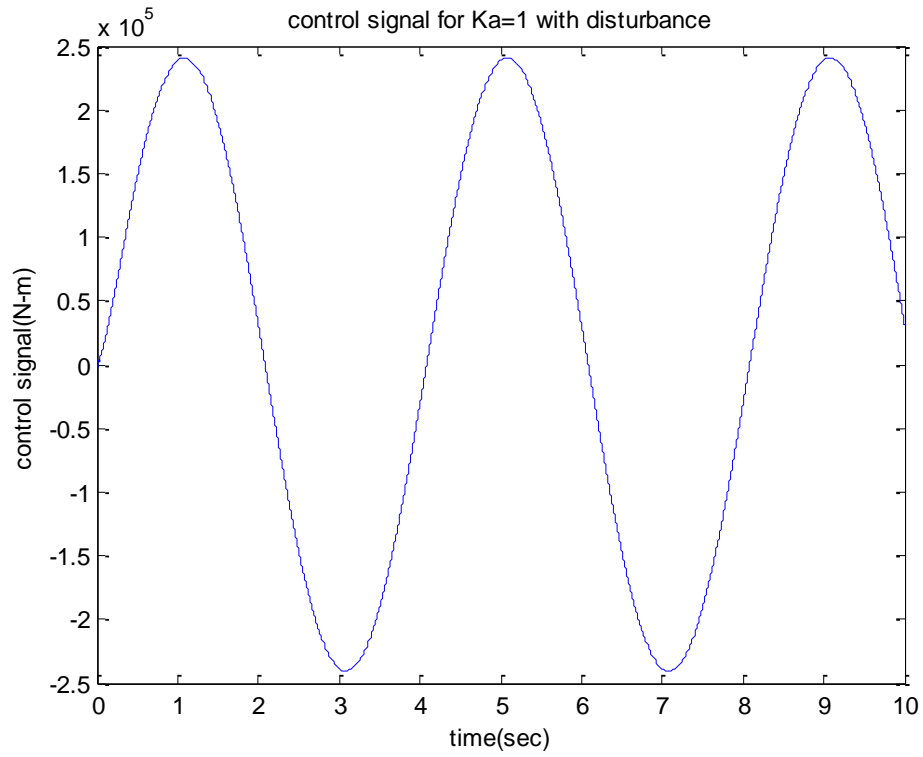
Figure 22 shows the control signal as K_a is 1.

Figure 22: Control signal as Ka=1

Figure 23 shows the output signal following the reference signal. We can see that the disturbance signal at 8.5th sec has small effect on output which is explored in figure 24.
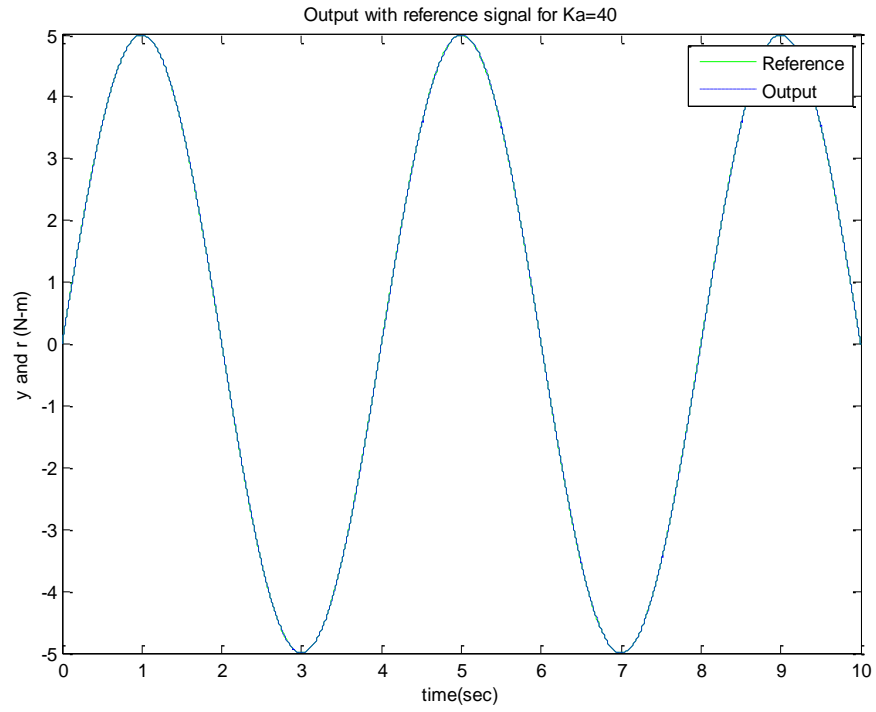
Figure 23: Output signal as K_a=40

Figure 24 shows the oscillations at the output of the EPAS caused by disturbance signal at 8.5th sec.
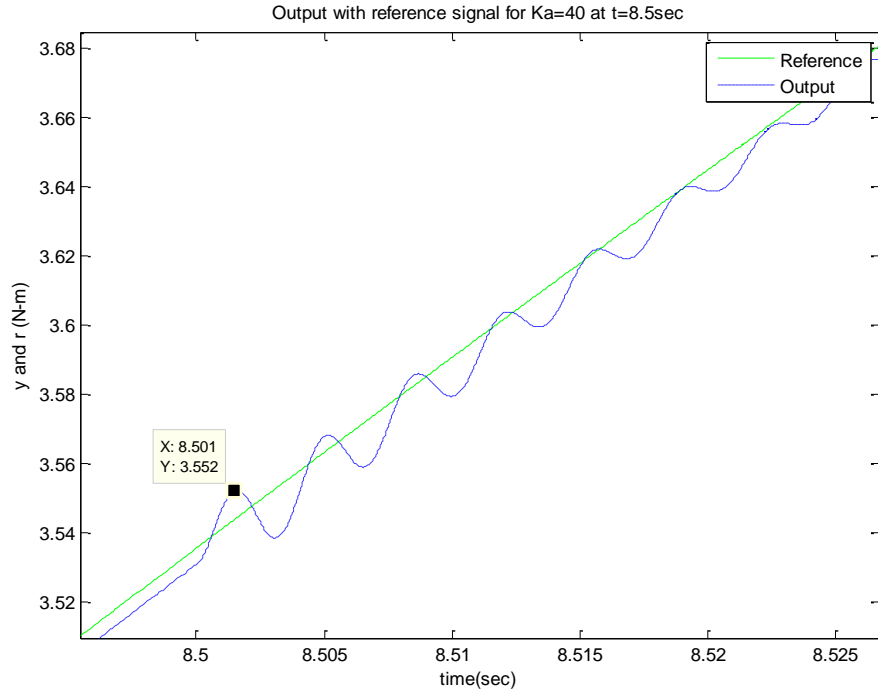
Figure 24: Output signal at 8.5th sec with K_a=40

Figure 25 shows the control signal as K_a is 40. We could observe that the amplitude of the control signal decreases from that of the control signal as K_a=1. Also, the effect (oscillations) of disturbance is clearly seen in this control signal.
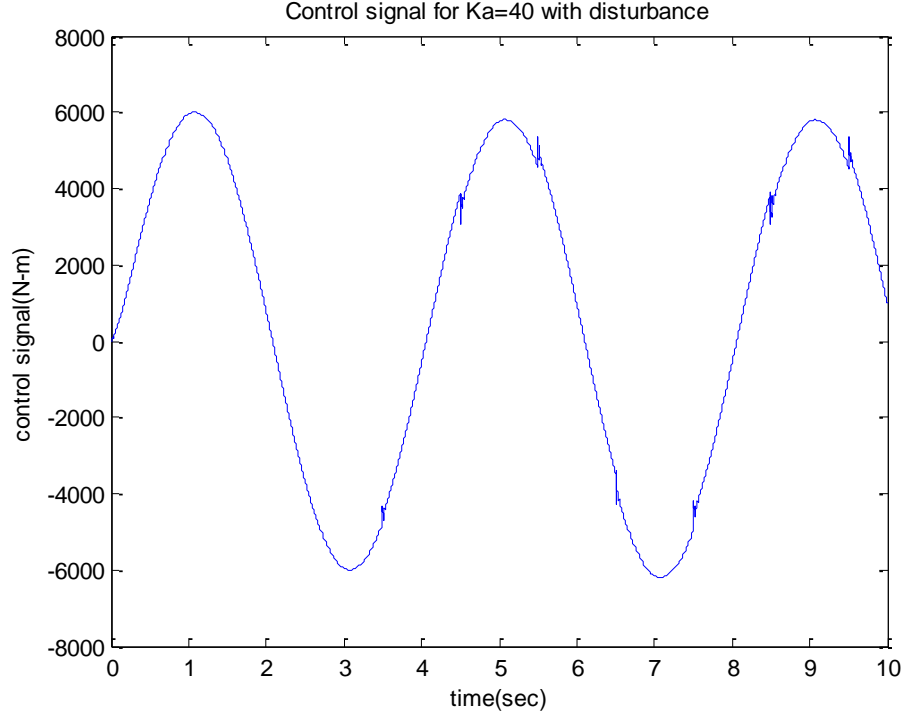
Figure 25: Control signal as *Ka*=40

5.2. Robustness

Figures 26, 28, 30 and 32 show the output signals of the ADRC controlled EPAS system in the presence of the disturbance (shown in Figure 19) as the controller bandwidth ω_c= 8000 *rad/s*. From these figures, we can see that the controller successfully compensated the disturbance since the output is identical to the reference signal. Figures 27, 29, 31 and 33 show the control efforts in the presence of the disturbance (given in Figure 19) as the controller bandwidth ω_c= 8000 *rad/s*. Figure 33 shows the control effort with

45

8% parameter variations in the presence of disturbance as ω_c=8000 rad/s and K_a=40. From the Figure 33, we can see that the control signal is much better compared to the one with -8% parameter variations.

Figure 26: Output with -8% parameter variations in the presence of disturbance as ω_c=8000 *rad/s* and K_a=1

Figure 27: Control signal with -8% parameter variations in the presence of disturbance as

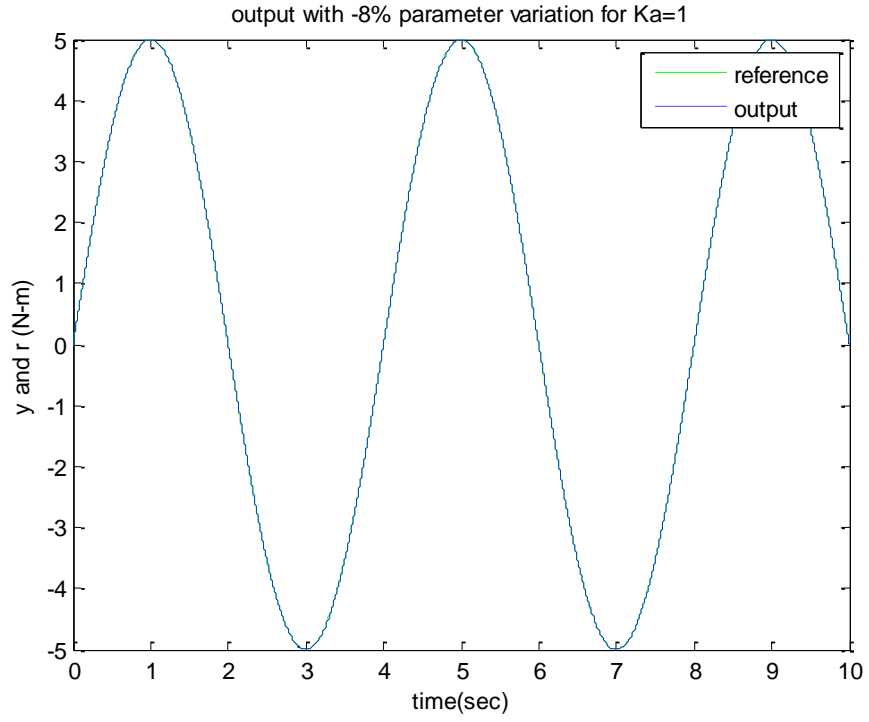ω_c=8000 *rad/s* and K_a=1

Figure 28: Output with -8% parameter variations in the presence of disturbance as

ω_c=8000 *rad/s* and K_a=40

Figure 29: Control signal with -8% parameter variations in the presence of disturbance as

ω_c=8000 *rad/s* and *Ka*=40

Figure 30: Output signal with 8% parameter variations in the presence of disturbance as

ω_c=8000 *rad/s* and K_a=1
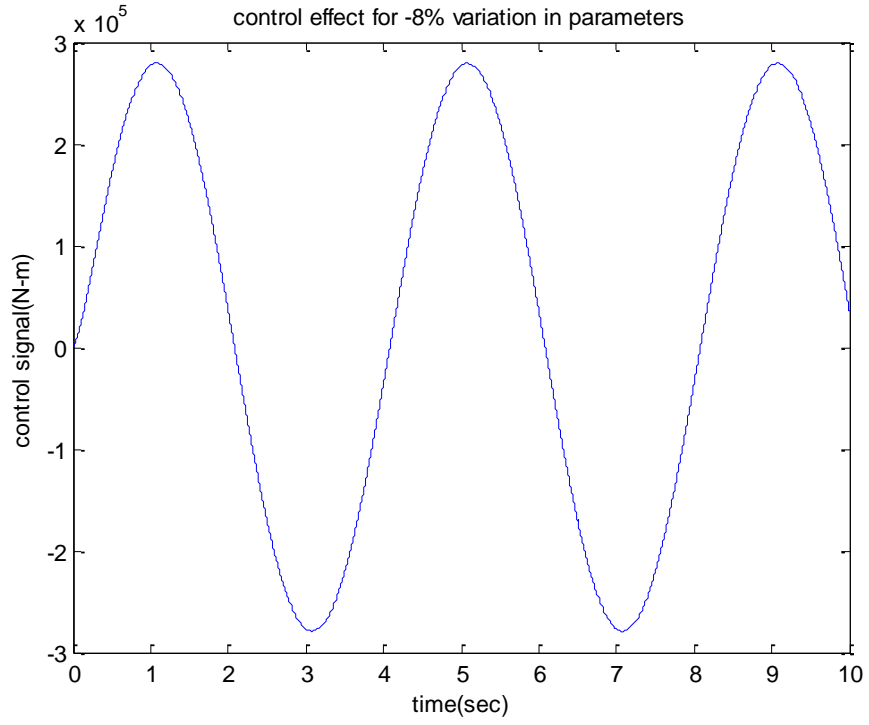
Figure 31: Control signal with 8% parameter variations in the presence of disturbance as
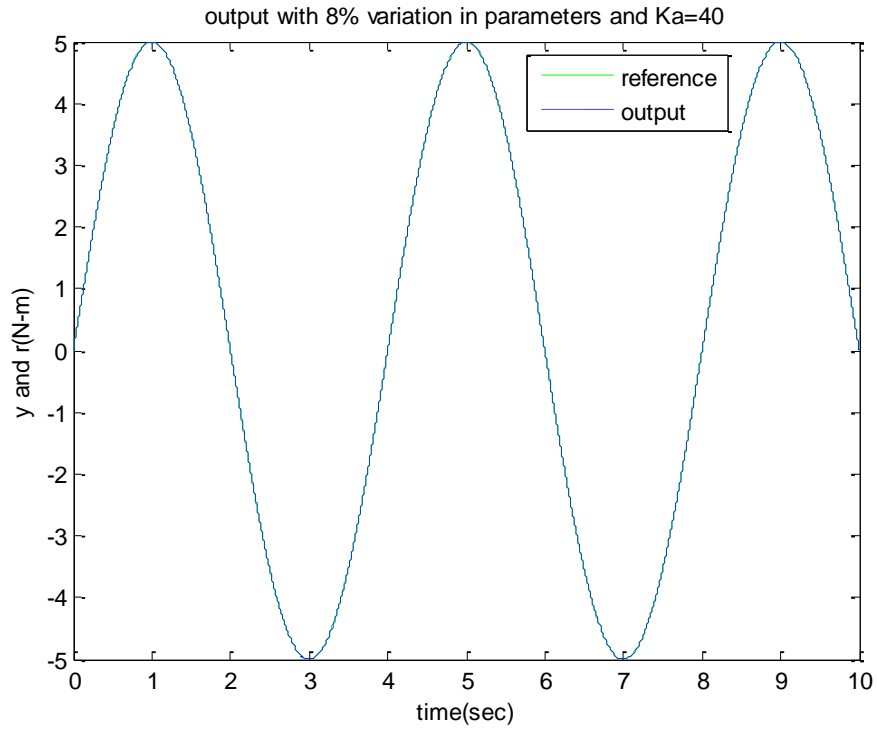
ω_c=8000 rad/s *and* K_a=1

Figure 32: Output signal with 8% parameter variations in the presence of disturbance as

ω_c=8000 *rad/s* and K_a=40
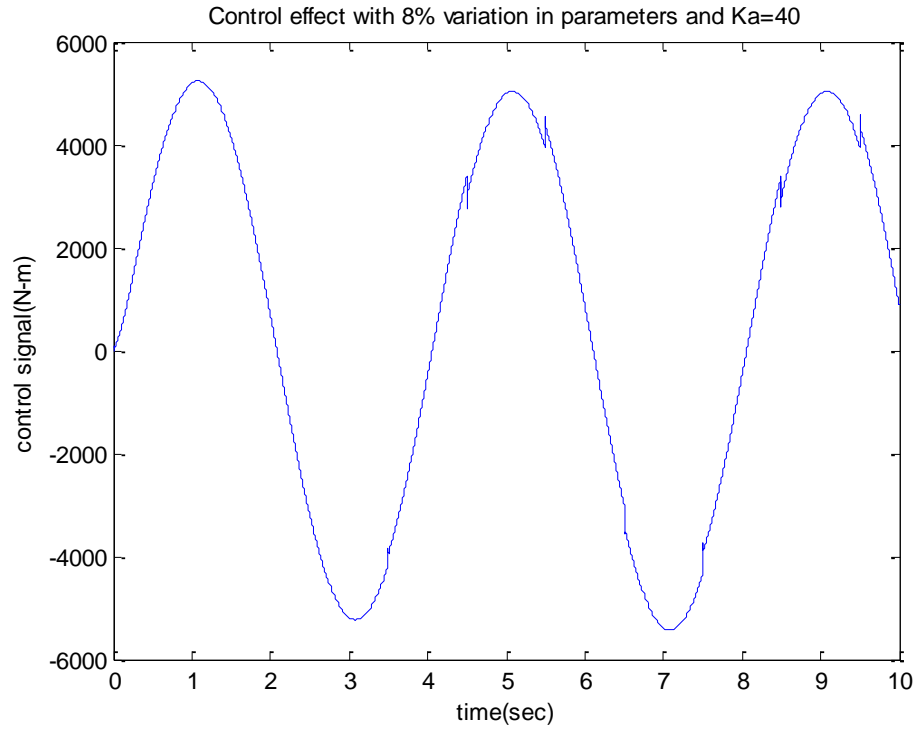
Figure 33: Control signal with 8% parameter variations in the presence of disturbance as
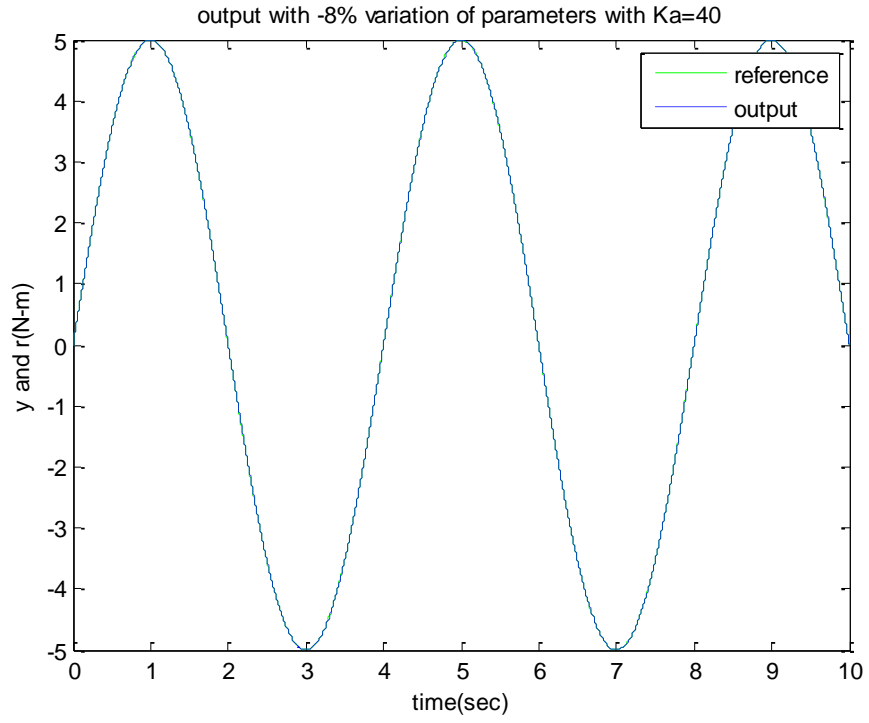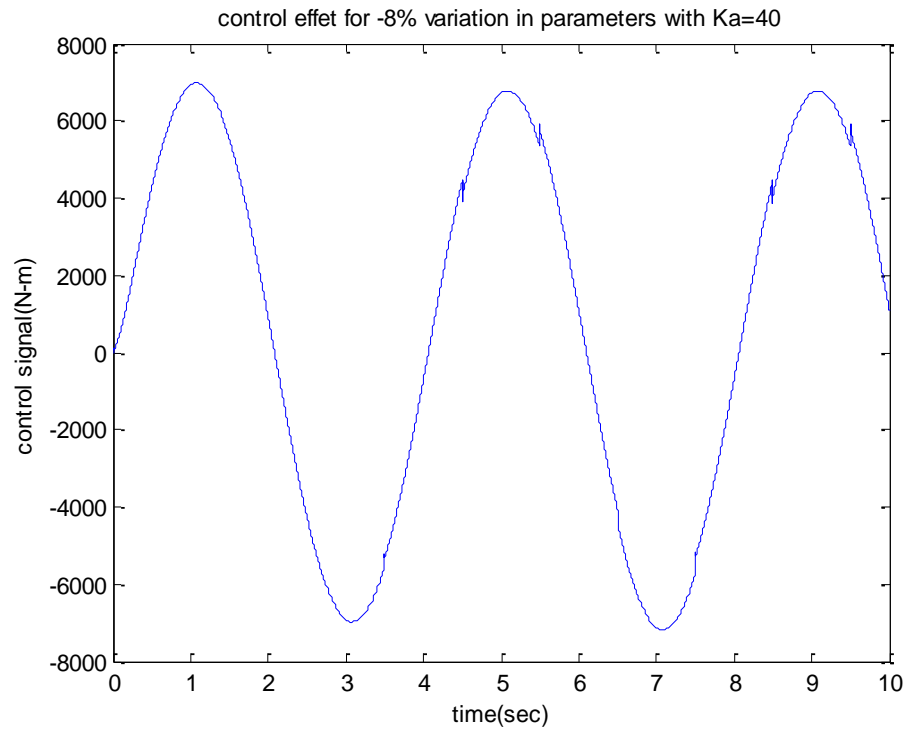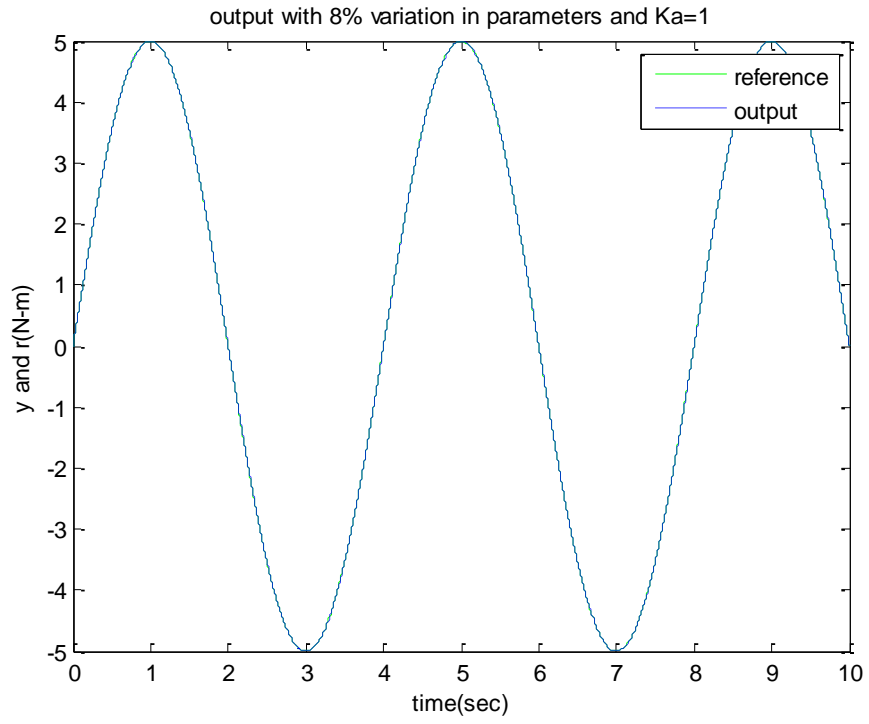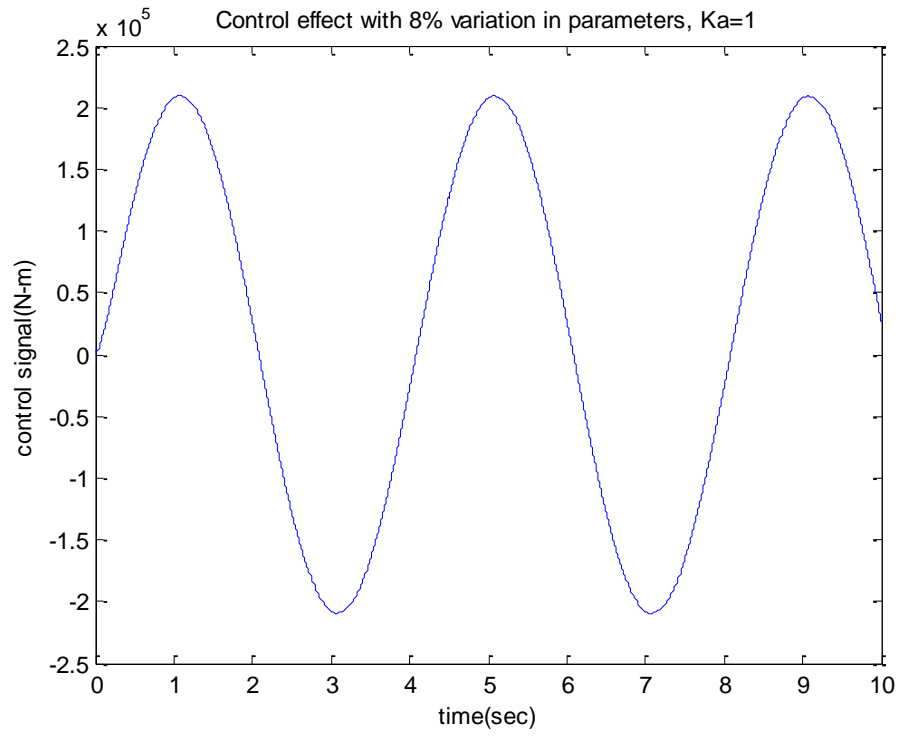
ω_c=8000 *rad/s* and K_a=40

CHAPTER VI

CONCLUSIONS AND FUTURE WORK

6.1. Conclusions

This thesis used an ADRC controller to solve the control problems in an EPAS system. The problems include disturbance rejection, system stabilization, and active compensation for modeling uncertainties which are inherent in the EPAS system.

Specifically a linear ADRC is designed in the thesis which has two tuning parameters "ω_c" and "ω_o" that are controller bandwidth and observer bandwidth. For simplicity, the tuning parameters are reduced to one by just equating the ω_o to five times of ω_c. The one-tuning parameter not only simplified the tuning process, but also makes the controller easy to implement in the real world.

The frequency domain analysis proves the controller to be one of practical controllers applied to the EPAS. The steady state error, the loop gain frequency response, the external disturbance rejection, the robustness, the stability margins demonstrate that

the ADRC is one of the effective controllers applied to EPAS for addressing the control issues such as disturbance rejection, system stabilization, and being robust against parameter uncertainties of EPAS. The simulation results demonstrate the ADRC has successfully driven the output torque to the desired torque in the presences of external disturbances, system uncertainties, and extreme speed conditions (as $K_a = 1$ and 40).

6.2. Future research

In the future, hardware implementation of the ADRC controlled EPAS is expected to be completed. We also plan to test this control system by conducting real-world road test. The application of ADRC will be extended to ball-bearing EPAS besides the column-type EPAS used in the thesis. ADRC could also be implemented to other subsystems of the automobile like cruise control, braking system, automatic transmission etc. In addition to automobile steering, the ADRC could also be employed to trucks steering.

REFERENCES

1. J. Kim, J. Song, "Control Logic for an Electric Power Steering System Using Assist Motor," *Mechatronics,* vol. 12, no. 3, pp. 447-459, Apr. 2002.

2. T. P. Newcomb, R. T. Spurr. "Steering," *A Technical History of the motor car*. New York: Adam Hilger, 1989, pp. 312.

3. Donald Bastow. *Car Suspension and Handling*, 2nd edition, London: Pentech Press, 1987.

4. M. G. Lay, James E. Vance. "A Surge of Power," in *Ways of the World: A History of the World's Road and of the Vehicles That Used Them*," New Brunswick, New Jersey: Rutgers University Press, 1992, pp.154.

5. Herbert E. Ellinger, Richard B. Hathaway. "Steering gears," in *Automotive Suspension, Steering, and brakes* Prentice-Hall, 1980, pp. 277-289.

6. J. Baxter, A.E. Bishop, "Analysis of Stiffness and Feel for a Power-Assisted Rack and Pinion Steering Gear," *SAE Paper, International Congress and Exposition,* Detroit, Michigan, pp. 880706, Feb 1988.

7. A.B. Proca, A. Keyhani, "Identification of Power Steering System Dynamic Models," *Mechatronics,* vol. 8, Issue 3, pp. 225-270, April 1998.

8. G. L. Nikulin and G. A. Frantsuzova, "Synthesis of an Electric-power steering control system," *Optoelectronics, Instrumentation and Data Processing,* vol. 44, no. 5, pp. 454-458, 2008.

9. H. Akhondi, J. Milimonfared, "Performance Evaluation of Electric Power Steering with IBM Motor and Drive System," in *Proc. Of IEEE region 8 International Conference on Computational Technologies in Electrical and Electronics Engineering,* Novosibirsk. Jul. 2008. pp. 175-179.

10. J. Song, K. Boo, H. S. Kim, J. Lee, and S. Hong. "Model Development and Control Methodology of a New Electric Power Steering System," *Journal of Automobile Engineering, v*ol. 218, pp.967-975, 2004.

11. Y. Morita, K. Torii, N. Tsuchida, et al.., "Improvement of Steering feel of Electric Power Steering System with Variable Gear Transmission System Using Decoupling Control," in *proc. of 10th IEEE International Workshop on Advanced Motion Control,* Trento, Italy, Mar. 2008, pp. 417-422

12. H. Zang, M. Liu, "Fuzzy Neural Network PID Control for Electric Power steering System," in *Proc. of IEEE International Conference on Automation and Logistics,*Jinan, China,Aug. 2007, pp. 643-648.

13. J. Lee, H. Lee, J. Kim, and J. Jeong, "Model Based Fault detection and Isolation for Electric Power Steering System," in *Proc. of International Conference on Control, Automation and System,* Seoul, Korea, Oct. 2007, pp. 2369-2374.

14. A.T. Zaremba, M.K. Liubakka, R.M. Stuntz, "Vibration Control Based on Dynamic Compentation in an Electric Power Steering System," in *Proc. of the first International Conference on Control of Oscillations and Chaos,* vol. 3, St. Petersburg, Russia, Aug. 1997, pp. 453-456.

15. A.T. Zaremba, M.K. Liubakka, R.M. Stuntz, "Control and Steering Feel Issues in Design of an Electric Power Steering System," in *Proc. of the American Control Conference,* Philadelphia, PA, Jun. 1998, pp. 36-40.

16. A.T. Zaremba, R.I. Davis, "Dynamic Analysis and Stability of a Power Assist Steering System," in *Proc. of the American Control Conference,* Seattle, Washington, Jun. 1995, pp. 4253-4257.

17. R.C. Chabaan, L.Y. Wang, "Control of Electrical Power Assist Systems: H^{∞} Design, Torque Estimation and Structural Stability," *JSAE Review,* vol. 22*,* Issue 4, pp.435-444. Oct. 2001.

18. X. Chen, T. Yang, X. Chen, K. Zhou, "A Generic Model Based Advanced Control of Electric Power Assisted Steering Systems," *IEEE Transaction on Control Systems Technology,* vol. 16, no. 6, Nov. 2008, pp. 1289-1300.

19. Z. X. Ping, L. Xin, C. Jie, M.J. Lai, "Parametric design and application of steering characteristic curve in control for electric power steering," *Mechatronics*, vol. 19, issue 6, pp. 905-911, 2009.

20. S. Haggag, A. Rosa, K. Huang, S. Cetinkunt, "Fault tolerant real time control system for steer- by- wire electro- hydraulic systems*,"Mechatronics*, vol. 17, Issue 2-3, pp. 129-142, March-April 2009.

21. A.R. Hanzaki, P.V.M. Rao, S.K. Saha, "Kinematic and sensitivity analysis and optimization of planar rack-and-pinion steering linkages*," Mechanism and Machine theory*, vol. 44, Issue 1, pp. 42-56, Jan. 2009.

22. Y.G. Cho, "Vehicle Steering Returnability with Maximum steering Wheel Angle at Low Speeds," *International Journal of Automotive Technology,* vol. 10, no. 4,pp. 431-439, 2009.

23. S. Nishimura, T. Matsunaga, "Analysis of response lag in hydraulic power steering system," *JSAE Review,* vol. 21, Issue 1, pp. 41-46, Jan. 2000.

24. M. Eksioglu, K. Kizilaslan, "Steering-wheel grip force characteristics of drivers as a function of gender, speed and road condition,"*International Journal of Industrial Ergonomic,* vol. 38, Issue 3-4, pp. 354-361, March-April 2008.

25. Xiang Chen, Xiaoqum Chen, and Ke Li. "Robust Control of Electric power-Assisted Steering System," *Vehicle Power and propulsion,* in *Proc. ofIEEE Conference,* Chicago, IL. Sep. 2005, pp. 473-478.

26. Peilin Shi, ShixiangGao and Yi Wang, "Research on Electric Power Steering System based on Compound Control of CMAC and PID," in *Proc. of2nd International symposium on Intelligent Information Technology and Security Informatics,*Moscow, Jan. 2009, pp. 39-41.

27. Jiang Hao-bin, Zhao Jing-bo, Liu hai-mei and Chen long, "Low-pass Filter Based Automotive EPS Controller and Comparative Full-vehicle Tests," in *Proc. of IEEE Control and Decision Conference,* Cancun, Mexico. Dec. 2008. pp. 4662-4665.

28. Anthony W. Burton, "Innovation Drivers for Electric Power-Assisted Steering," *IEEEControl Systems Magazine,* vol. 23, Issue 6, pp. 30-39, Dec. 2003.

29. J. Han, "From PID to Active Disturbance Rejection Control," *IEEE Transactions on Industrial Electronic,* vol. 56, no. 3, pp. 900-906, Mar. 2009,

30. Z. Gao, "Active Disturbance Rejection Control: A Paradigm shift in Feedback Control Design," in *proc. of American Control Conference,* Minneapolis, MN, Jun. 2006, pp. 2399-2405.

31. Z. Gao, Y. Huang, J. Han, "An alternative paradigm for control system design," in *proc. of IEEE Conference on Decision and Control,* Orlando, FL. vol. 5, Dec. 2001, pp. 4578-4585.

32. Z. Gao, "Scaling and Parameterization Based Controller Tuning," in *proc. of the 2003 American Control Conference,* Denver, Colorado. vol. 6, Jun. 2003. pp. 4989-4996.

33. L. Dong, D. Avanesian, "Drive-mode Control for Vibrational MEMS Gyroscope," *IEEE Transaction on Industrial Electronics,* vol. 56, no. 4, pp. 956-963, April 2009.

34. L. Dong, Q. Zheng, and Z. Gao, "On Control System Design for the Conventional Mode of Operation of Vibrational Gyroscope," *IEEE Sensors Journal,* vol. 8, no. 11, pp. 1871-1878, Nov. 2008.

35. G. Tian, Z. Gao, "Frequency Response Analysis of Active Disturbance Rejection Based Control System," in *proc. of IEEE International Conference on Control Applications,* Singapore, Oct. 2007, pp. 1595-1599.

36. L. Dong, P. Kandula, Z. Gao, D. Wang, "On a Robust Control System Design for an Electric Power Assist Steering System", in *Proceedings of 2010 American Control Conference,* Baltimore, MD, Jul. 2010.

APPENDICES

System parameters of EPAS

Stiffness coefficient of steering column: K_s=115

Steering column Pinion Radii: R_s=0.00778

Moment of inertia of steering column: J_s=0.04

Damping coefficient of Steering column: b_s=0.36

Gear ratio: G=7.225

Mass of rack: m=32.1

Moment of inertia of assist motor: J_m=0.0004707

Assist pinion radii: R_m=0.00778

Damping coefficient of rack: b=650*2.1 = 1365

Damping coefficient of the assist subsystem: b_m=0.00334*2.1

Stiffness coefficient of rack: K_T=80000

Effective rack mass: m_e=m+G*G*J_m /(R_m *R_m) = 438.04

Effective damping coefficient: b_e=b+G*G*b_m /(R_m *R_m) = 7413.98

Effective stiffness coefficient: K_e=K_T +K_s /(R_s *R_s) = 1980000

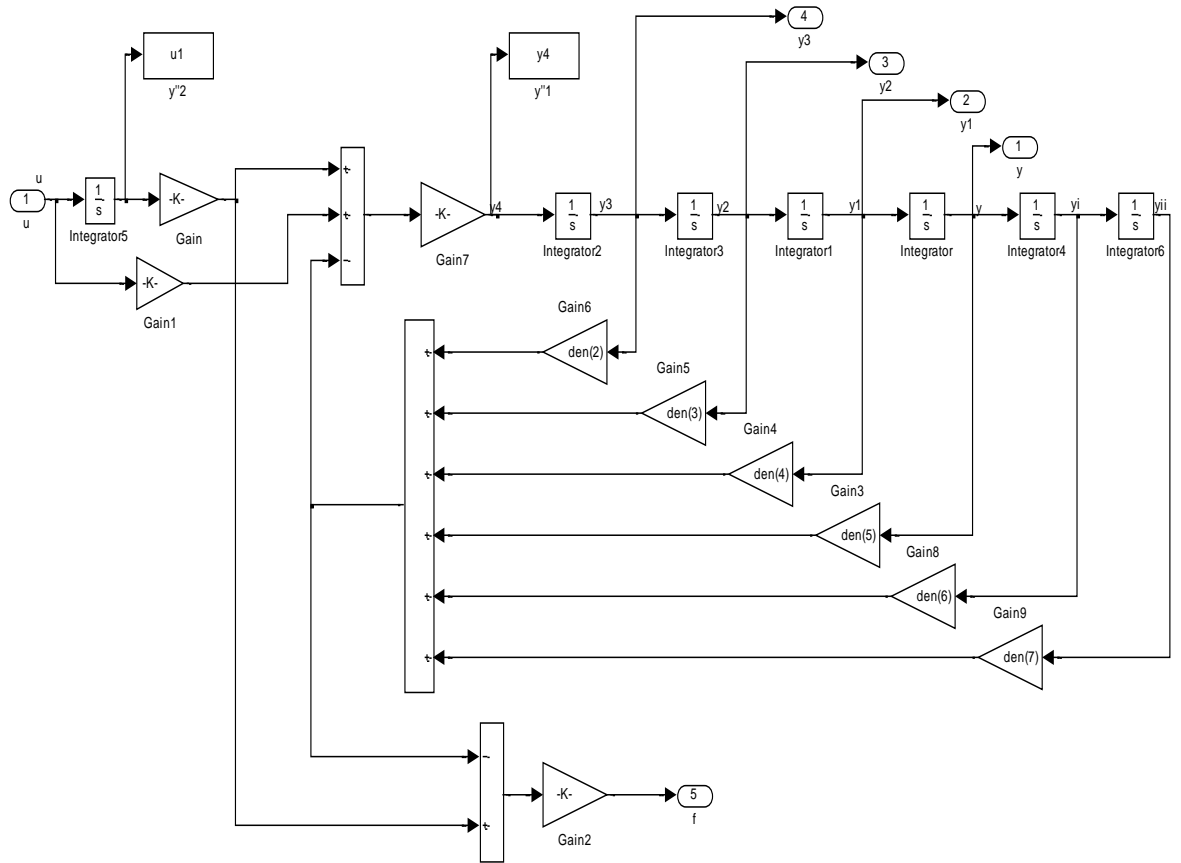Low-pass filter coefficients: P_t=90π and P_a=200π.

Figure A: Simulink model of the EPAS *(G(s))*
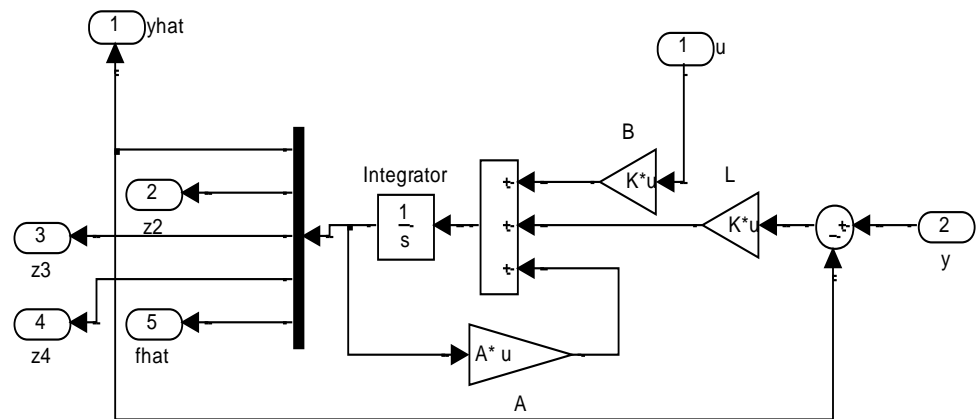
Figure B: Simulink Model of the ADRC controlled EPAS

Figure C: Simulink Model of the ESO (ESO_continous)